NASA TECHNICAL NOTE

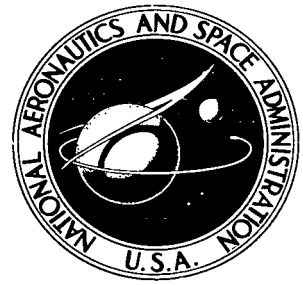

NASA TN D-6624

NASA TN D-6624

A STUDY OF THE EFFECT OF SELECTED MATERIAL PROPERTIES ON THE ABLATION PERFORMANCE OF ARTIFICIAL GRAPHITE

by Howard G. Maahs

Langley Research Center
Hampton, Va. 23365

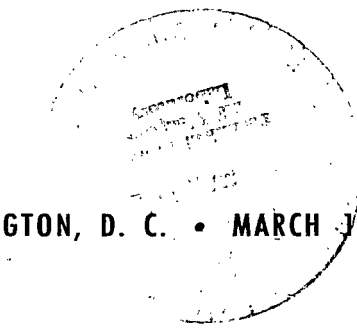

NATIONAL AERONAUTICS AND SPACE ADMINISTRATION • WASHINGTON, D. C. • MARCH 1972

1. Report No.	2. Government Accession No.	3. Recipient's Catalog No.
NASA TN D-6624		

4. Title and Subtitle	5. Report Date
A STUDY OF THE EFFECT OF SELECTED MATERIAL PROPERTIES ON THE ABLATION PERFORMANCE OF ARTIFICIAL GRAPHITE	March 1972
	6. Performing Organization Code
7. Author(s)	8. Performing Organization Report No.
Howard G. Maahs	L-8085
	10. Work Unit No.
9. Performing Organization Name and Address	970-32-20-13
NASA Langley Research Center Hampton, Va. 23365	11. Contract or Grant No.
	13. Type of Report and Period Covered
12. Sponsoring Agency Name and Address	Technical Note
National Aeronautics and Space Administration Washington, D.C. 20546	14. Sponsoring Agency Code

15. Supplementary Notes

16. Abstract

Eighteen material properties have been measured on 45 different, commercially available, artificial graphites. Ablation performance of these same graphites was also measured in a Mach 2 airstream at a stagnation pressure of 5.6 atm. Correlations were developed, where possible, between pairs of the material properties. Multiple regression equations were then formulated relating ablation performance to the various material properties, thus identifying those material properties having the strongest effect on ablation performance. These regression equations reveal that ablation performance in the present test environment depends primarily on maximum grain size, density, ash content, thermal conductivity, and mean pore radius. For optimization of ablation performance, grain size should be small, ash content low, density and thermal conductivity high, and mean pore radius large.

17. Key Words (Suggested by Author(s))	18. Distribution Statement
Ablation Graphite Carbon	Unclassified – Unlimited

19. Security Classif. (of this report)	20. Security Classif. (of this page)	21. No. of Pages	22. Price*
Unclassified	Unclassified	58	$3.00

*For sale by the National Technical Information Service, Springfield, Virginia 22151

A STUDY OF THE EFFECT OF SELECTED MATERIAL PROPERTIES ON THE ABLATION PERFORMANCE OF ARTIFICIAL GRAPHITE

By Howard G. Maahs
Langley Research Center

SUMMARY

A total of 18 material properties have been measured on 45 different, commercially available, artificial graphites. A correlation based on 10 of these graphites was developed, permitting the difficult-to-measure property, thermal conductivity, to be predicted in terms of the easier-to-measure property, electrical conductivity. Other correlations between pairs of the 18 graphite material properties have been developed where possible, reducing the original 18 material properties to 10 mutually independent properties. Ablation performance (as determined by total length change during test, recession rate, surface temperature, surface texture, and degree of gouging) was measured on the same 45 graphites in a nominal Mach 2 airstream having a nominal enthalpy of 2.17 MJ/kg and a stagnation pressure of 5.6 atm. Nominal heating rates were 513 W/cm^2.

Multiple regression equations were formulated relating ablation performance to the reduced set of 10 independent material properties, thereby identifying those material properties having the most pronounced effect on ablation performance in the present test environment. These properties are maximum grain size, density, ash content, thermal conductivity, and mean pore radius. For optimization of ablation performance, grain size should be small, ash content low, density and thermal conductivity high, and mean pore radius large. Maximum grain size should be kept below 0.22 mm to insure a smooth graphite surface during ablation.

The method of stepwise multiple regression employed in this study for determining which properties are important in affecting ablation performance has been shown to be both powerful and efficient. Its soundness is demonstrated by the fact that it properly predicts ablation performance to be related to certain material properties known from theoretical or experimental considerations to affect ablation performance. In order to determine other material properties which might also have an important effect on ablation performance, a more extensive list of properties than the 18 considered here could be employed.

It is of some additional interest that, in the course of the present investigation, Graph-i-tite "G" graphite was found to be more erosion resistant than the usual standard

of comparison, ATJ graphite. Of the two forms of Graph-i-tite "G," the large-grained form eroded with a rough surface while the fine-grained form eroded with a smooth surface. Accordingly, the fine-grained form of Graph-i-tite "G" appears attractive for future study.

INTRODUCTION

Carbon is a unique material existing in a wide variety of forms: natural graphite, carbon black, industrial artificial graphite, and more recently, the pyrolytic carbons and graphites and the glass-like carbons. Although all except natural graphite are artificial in the sense that they are manufactured, the term "artificial graphite" is commonly reserved for the conventional industrial graphite fabricated from carbonaceous filler and binder materials and subsequently graphitized.

Artificial graphite has been of particular interest for some time as an ablation material because of its many desirable structural and thermal properties at high temperatures, as well as its machinability and ease of fabrication into relatively large pieces. However, a detailed understanding of this material and its performance in various applications is severely complicated because it is fabricated in many forms by a wide variety of proprietary formulations and techniques. Furthermore, each manufacturer usually produces a broad line of artificial graphites, each intended for different applications. Because of these complications, there exists to date no simple, meaningful way to select, from the hundreds of artificial graphites manufactured, the ones best suited for a particular use, such as for ablation materials. Also, because of the proprietary nature of these artificial graphites, there is even no way by which any two graphites can be determined to be fully equivalent, whether produced by the same manufacturer or not.

In an attempt to resolve this problem, it was reasoned that if the primary fundamental physical, chemical, and structural properties, as well as ablation performance, were determined for a large number of different graphites then possibly some dependence of ablation performance on the fundamental properties could be found. This information would aid in selecting particular graphites for consideration in ablation applications, but would be of greatest value in establishing the prime collection of properties desirable to fabricate into a graphite in order to optimize its ablation performance.

Some of this basic property information is already available. Chemical impurity data are available in reference 1 on 40 selected grades of commercially available artificial graphite, with the impurities grouped by reported effect on oxidation rate, that is, whether catalytically accelerating or inhibiting. (Ref. 1 indicates that the combined effect of the natural impurities in graphite should be accelerating, and this is confirmed experimentally in ref. 2 for four graphites differing greatly in impurity content, grain size, and

density.) Crystallographic data on crystallite sizes and lattice dimensions are presented in reference 3 for the same 40 artificial graphites studied in reference 1.

The purpose of the present investigation is to measure for a wide variety of artificial graphites those additional material properties which are suspected of having potentially large effects on ablation performance, to determine the ablation performance of these same graphites, and to relate ablation performance to the measured properties. A second purpose is to develop correlations, where possible, between pairs of the graphite material properties themselves.

In this report are presented measurements of physical, chemical, and structural properties of 45 commercially available artificial graphites. These properties include density, maximum grain size, ash content, thermal conductivity, interlayer spacing of the filler carbon, and measurements of internal volume, surface area, and pore radii. Correlations between pairs of these properties have been made where appropriate. Also presented for these same graphites are the following ablation-performance data: total length change, stagnation-point recession rate, steady-state stagnation-point surface temperature, surface texture, and degree of gouging. These ablation data are analyzed in light of the material-property data, with multiple regression equations being formulated which relate ablation performance to them.

SYMBOLS

A_p	pore area, m^2/g
$\overline{A}$	ash content, ppm
a	lattice dimension in the a direction, Å
a_i	coefficient
b_i	coefficient
c	constant
d_c	interlayer spacing of the filler carbon, Å
G_m	maximum grain size, mm
i	index

k	thermal conductivity, W/cm-K
P	pressure, N/m^2
R	pore radius, μm
R_p	most probable pore radius, μm
$\bar{R}$	average absolute percent residual (or deviation) about regression
r	pore radius in the micropore region, Å
r_a	average pore radius, Å
r_m	mean pore radius, Å
r_p	most probable micropore radius, Å
S	surface area, m^2/g
$\dot{s}$	linear recession rate at the stagnation point, cm/sec
T	stagnation-point surface temperature at steady state, K
V_p	total pore volume, cm^3/g
v	cumulative volume in pores up to pore radius r, cm^3/g
v_p	pore volume, cm^3/g
x_i	i^{th} material property
y	a general ablation performance parameter
Γ	degree of gouging
Δl	total specimen length change resulting from a 30-second exposure to the test environment, cm

ϵ	total void porosity, percent
θ	contact angle between mercury and graphite, degrees
θ_{air}	air-open void porosity, percent
θ_{Hg}	mercury-open void porosity, percent
ρ_{air}	air displacement density, g/cm^3
ρ_P	bulk density, g/cm^3
ρ_T	theoretical density, g/cm^3
σ	surface tension, N/m
σ_E	electrical conductivity, $(\Omega\text{-cm})^{-1}$
τ	surface texture

DESCRIPTION OF MATERIALS

The particular artificial graphites considered in the present study were intentionally selected to include a wide range of material properties. These graphites are listed in table I. All are commercially available. Several were obtained from the manufacturers in a specially purified form (presumably purified by high-temperature halogenation) in addition to the conventionally supplied form and are noted in table I by the letters "GP" appended to the standard grade designation. With the exception of graphites AHDG, AGSX, AGOT, and the Graph-i-tite grades, which were fabricated by extrusion, all of the graphites were fabricated by molding.

Specimens for the material-property and ablation-performance measurements were drawn at random from as-supplied graphite billets obtained directly from the manufacturers. The required specimens for each particular graphite were drawn from the same production batch, and, in all but a few cases, were drawn from a single billet. Prior to cutting the specimens from a billet, the billet was trimmed to eliminate the possibility of nonrepresentative skin effects confusing the subsequent material-property or ablation-performance measurements. Replicate measurements of the material properties on different specimens of the same graphite yielded no unreasonable variations in measured values.

MATERIAL-PROPERTY MEASUREMENTS

Bulk Density

Bulk density ρ_P was determined from the mass of a graphite specimen divided by its volume. Specimen mass was measured with an analytical balance, and specimen volume was calculated from the dimensions of an accurately machined specimen. Specimen volume was on the order of 3 cm^3. Measurements were made on three specimens of each graphite and the results averaged.

Air Displacement Density

Air displacement density ρ_{air} was determined as the mass of a specimen divided by the volume of the solid in the specimen displacing air at 2 atm. Mass was measured by an analytical balance, and the solid volume was measured with a gas pycnometer (Beckman Instruments, Inc., Model 930). Three specimens of each graphite were measured and the results averaged.

Theoretical Density

The theoretical density ρ_T is defined as the true density of the graphite crystal, and therefore depends on the lattice dimensions a and d_c. Nightingale (ref. 4) gives an expression for the theoretical density $\rho_T = 91.93/2a^2d_c$. The lattice dimension a was shown in reference 3 to be a constant at 2.4614 Å. Substitution of this value reduces the expression for theoretical density to $\rho_T = 7.587/d_c$. The interlayer spacing d_c was obtained from reference 3.

Total Pore Volume

The total pore volume V_p is a specific pore volume defined as the volume of mercury which can be intruded into the pores of the graphite specimen at a pressure of 103.4 MN/m^2 (15 000 psia) divided by the mass of the specimen. All mercury intrusion measurements were made on a mercury porosimeter and were performed by the American Instrument Co., Inc., on samples furnished by the National Aeronautics and Space Administration. Total pore volume was measured on two specimens of each graphite, and the results were averaged.

Most Probable Pore Radius

The most probable pore radius R_p is defined as that pore radius at which occurs the greatest volume increment of mercury intruded into the graphite per increment in pore radius. The experimental data are obtained with a mercury porosimeter, with the pore radius being related to the applied intrusion pressure P by the equation

$R = -2\sigma \cos \theta/P$ where σ is the surface tension of mercury and θ is the contact angle between mercury and graphite. Taking $\sigma = 480 \times 10^{-3}$ N/m and $\theta = 140^{o}$ (ref. 5) there results $R = 735.4 \times 10^{3}/P$ where P is in N/m^2 and R is in μm. Plots of mercury intrusion volume as a function of intrusion pressure were prepared by the American Instrument Co., Inc., on samples furnished by NASA. Most probable pore radii R_p were obtained from these plots by the author. Since intrusion pressure ranged from about 13.8 kN/m^2 (2 psia) to 103.4 MN/m^2 (15 000 psia), the distribution of radii observable lies between approximately 0.007 μm and 53 μm. Reported results are the average of measurements on two samples.

Maximum Grain Size

The maximum grain size G_m is the maximum particle size of the filler carbon used in the manufacture of the artificial graphite, as conventionally determined by screening. The maximum grain size was obtained from the manufacturers.

Pore Volume

Pore volume v_p is a specific volume defined as the void volume in pores having radii less than or equal to 300 Å per unit mass of the specimen. It was determined from the nitrogen adsorption isotherms of the graphites by the method of Barrett, Joyner, and Halenda (ref. 6). Although nitrogen has a molecular diameter on the order of 3 Å (ref. 7), as a practical matter, the lower limit of the pore radii included in the volume measurement by this method is about 7 Å. The generation of the adsorption isotherms and the calculation of pore volume were performed by the American Instrument Co., Inc., on specimens supplied by NASA. Measurements for each graphite were made on two specimens and the results averaged.

Pore Area

The pore area A_p is a specific surface area defined as the surface area in pores having radii less than or equal to 300 Å per unit mass of the specimen. Pore area was calculated from the same nitrogen adsorption isotherms used to determine pore volume v_p by the American Instrument Co., Inc., according to the method of Barrett, Joyner, and Halenda (ref. 6). Measurements were made on two specimens and the results averaged.

Surface Area

Surface area S is the total solid surface area per unit mass as calculated from the first part of the nitrogen adsorption isotherm by the classical BET method (ref. 4). The same nitrogen adsorption isotherms used to determine v_p and A_p were used and

the American Instrument Co., Inc., performed the calculations. Results are the average of individual determinations on two separate specimens.

Average Pore Radius

The average pore radius r_a is defined as that pore radius which divides the pore volume distribution into two equal parts (ref. 8). It was calculated from the nitrogen adsorption isotherms of the specimens by the American Instrument Co., Inc. Measurements were made on two separate specimens and the results averaged.

Most Probable Micropore Radius

The most probable micropore radius r_p is defined as that pore radius at which occurs the greatest change of cumulative pore volume v per change in pore radius r. It is analogous to the most probable pore radius R_p with the difference being that the most probable micropore radius is determined from the nitrogen adsorption isotherms, whereas the most probable pore radius is determined from mercury porosimetry. (Recall that mercury porosimetry yields a pore radius distribution between 0.007 μm and 53 μm, and that nitrogen adsorption yields a radius distribution between 7 Å (0.0007 μm) and 300 Å (0.030 μm).) The most probable micropore radius was determined by the author from plots of dv/dr as a function of r prepared from the nitrogen adsorption isotherms of the specimens generated by the American Instrument Co., Inc. Results are the average of individual determinations on two separate specimens.

Mean Pore Radius

The mean pore radius r_m, an alternate definition of a characteristic pore dimension, is defined as $2v_p/S$, where v_p is the pore volume, and S is the surface area (ref. 8). It was computed from v_p and S as determined from the nitrogen adsorption isotherms. The results represent an average of two measurements, one on each of two samples.

Total Void Porosity

The total void porosity ϵ is defined as the ratio of total void volume – whether open (i.e., accessible to air) or closed (i.e., inaccessible to air) – to bulk volume. It is expressible in terms of the densities already discussed and was calculated from the formula $\epsilon = 1 - \rho_P/\rho_T$.

Air-Open Void Porosity

Air-open void porosity θ_{air} is defined as the ratio of void volume open to air to bulk volume. It was calculated from $\theta_{air} = 1 - \rho_P/\rho_{air}$.

Mercury-Open Void Porosity

Mercury-open void porosity θ_{Hg}, an alternate definition of open void porosity, is defined as the ratio of the void volume as measured by mercury intrusion to bulk volume. It differs from air-open void porosity in that more pore volume should be open to air than to mercury (in spite of the high mercury intrusion pressures). It was calculated from the mercury porosimetry data by the formula $\theta_{Hg} = \rho_P V_p$.

Ash Content

Ash content $\overline{A}$ is a relative measure of the concentration of chemical impurities present. Experimentally, it is the mass of residue remaining after complete combustion of the graphite, expressed in mass parts per million of the original graphite. Ash content is a convenient measure of the relative concentration of total elemental impurities in an artificial graphite (ref. 1). Except where noted, ash content was obtained from reference 1 where a breakdown of the total chemical impurities in the graphites into separate chemical elements is also given.

Interlayer Spacing

Interlayer spacing of the filler carbon d_c is a measure of the spacing between layer planes in the filler-carbon crystal lattice, and serves as a relative measure of the degree of graphitization, that is, the degree to which the filler crystal structure approaches that of a theoretically perfect crystal (d_c for a perfectly graphitized crystal is 3.354 Å). The interlayer spacing, measured by X-ray diffraction, was taken from reference 3.

Thermal Conductivity

Accurate measurement of the thermal conductivity k of graphite is both difficult and tedious. Reference 9 points out, however, that the thermal conductivity of a graphite is uniquely related to its electrical conductivity σ_E, and therefore can be predicted from it. This is a particularly valuable situation because accurate electrical conductivity data are relatively easy to obtain. Accordingly, the thermal conductivities of the present graphites were determined from experimental measurements of electrical conductivity. The equation used to relate these two parameters is given by

$$k = 1.513 \times 10^{-3} \sigma_E - 0.1388 \times 10^{-6} \sigma_E^2$$

and was specifically developed for the present graphites. Its development is given in appendix A. All measurements of electrical conductivity were made in the across-grain direction by a four-probe direct-current technique and were performed by the Oak Ridge National Laboratory on solid cylindrical samples furnished by NASA. This four-probe

technique uses direct-current leads brought into contact with the end faces of the cylindrical sample and knife-edges of known separation contacting the surface of the sample from which the potential drop along the specimen axis is obtained. Electrical conductivity measurements were made on three samples of each graphite and the results averaged.

ABLATION-PERFORMANCE MEASUREMENTS

Test Environment

The test environment consisted of a nominal Mach 2 airstream, with a nominal total enthalpy of 2.17 MJ/kg and a stagnation pressure of 5.6 atm (5.67×10^5 N/m^2). Heating rates were nominally 513 W/cm^2. This condition was obtained in the arc-heated materials jet at the Langley Research Center which is described in reference 10. Stagnation pressures and heating rates in the test stream were measured with a calibrated pressure probe and a calibrated Gardon foil asymptotic calorimeter, respectively. Stream enthalpies were calculated from the pressure and heating rate according to the theory of Fay and Riddell (ref. 11).

Test Specimens

The artificial graphite test specimens were machined from graphite billets as supplied by the manufacturer. Each specimen consisted of a 1.270-cm-diameter hemisphere-cylinder, 1.905 cm long, with a 0.635-cm nose radius. During an ablation test, the graphite test specimen was mounted in a 1.905-cm-long phenolic-asbestos insulator which was, in turn, mounted in a water-cooled holder (see fig. 1). All graphites were mounted so that the test stream impinged on the specimen normal to the preferred orientation of the basal plane surfaces (i.e., in the across-grain direction), although reference 2 demonstrates that this attention to orientation is not really necessary provided, as in the present case, that there is no efficient path for thermal conduction from the specimens. Only one ablation-performance test was made on each graphite.

Instrumentation and Data Analysis

The instrumentation used for measuring ablation response of the graphite specimens consisted of a bench micrometer (direct reading in inches to 0.0001 inch (0.00025 cm)), a motion-picture camera with a framing rate of 200 pictures per second, and a continuous recording photographic pyrometer, the theory and principle of which are described in reference 12. The parameters selected for evaluating ablation performance were total length change Δl resulting from a 30-second exposure to the test environment, linear stagnation-point recession rate $\dot{s}$, steady-state stagnation-point surface temperature T, surface texture τ, and degree of gouging Γ.

Total length change was obtained from length measurements of the specimen before and after test using the bench micrometer. Linear recession rate was determined from the motion-picture-film record of the eroding specimen as follows. Specimen length as a function of time was obtained from the film records of the specimen with the aid of a motion analyzer. These data were then plotted as shown in figure 2. Customarily, specimen length initially increased because of thermal expansion of the graphite, but soon passed through a maximum and thereafter decreased continuously because of erosion. Recession rate was taken to be the slope of the curve over the linear portion of the length decrease with time as determined by a least-squares fit of the data.

Steady-state stagnation-point surface temperature was determined from the motion-picture-film record taken with the photographic pyrometer. Stagnation-point surface temperatures as a function of time were obtained from this record and plotted as shown in figure 2. For determining these temperatures, the emissivity of graphite was taken to be 0.94 (refs. 13 and 14). The representative stagnation-point surface temperature was taken as the steady-state maximum temperature attained during the run. In all cases, this temperature was reached during the linear portion of the length-time curve.

Surface texture is a measure of the degree of small-scale unevenness or roughness of the surfaces of the after-test specimens, as assigned by visual inspection. Numbers range from 1 (smooth) to 3 (rough). Degree of gouging is a measure of the extent to which the after-test specimens showed gross material loss from their surfaces, as evidenced by gouges, grooves, or missing chunks of material. Numbers from 1 (no gouging) to 3 (severe gouging) were assigned by visual inspection. The numerical designations for both surface texture and degree of gouging were assigned in accord with the photograph of the representative after-test specimens shown in figure 3.

Typical Test Sequence

A typical experimental test sequence proceeded as follows. The magnetically rotated electric-arc air heater was started and 12 seconds were allowed for the arc to stabilize and the test-stream environment to become established. The motion-picture camera and photographic pyrometer were started and the test-stream heating rate was measured. The graphite specimen to be tested was inserted into the stream and allowed to remain for 30 seconds. After retraction of the specimen, a final heating-rate measurement was made. Each event in this sequence was executed automatically and controlled by a preset programmer.

EXPERIMENTAL RESULTS AND DATA ANALYSIS

The results of the material-property measurements and ablation-performance measurements are shown in table I. All data are complete on the first 40 graphites; however,

the last five were added during the experimental program and complete material-property data have not been obtained on them. Accordingly, in the following discussions regarding correlations of material properties and ablation performance, only the data on the first 40 graphites are considered.

In addition to the ablation test data shown in table I for the two Graph-i-tite "G" grades, separate tests were made to compare their ablation performance in more detail. These additional ablation-performance data are shown in table II and discussed in appendix B.

Material-Property Correlations

It is apparent from the description of the material-property measurements in the preceding section that, although conventional definitions of the properties were used, many of the properties ought to be closely related (i.e., such properties as pore area A_p and surface area S, the various alternate definitions of a characteristic pore dimension, etc.) Accordingly, it was deemed an important part of the present study to determine, where possible, correlations of these material properties, thus reducing the total number of property variables requiring consideration. In order to provide the maximum usefulness from this reduction, correlations were sought predicting the more-difficult-to-measure properties in terms of the simpler-to-measure properties. For instance, since the surface area S is simpler to measure than the pore area A_p (because only the first part of the adsorption isotherm is required to determine S), it is desirable to develop a correlation predicting A_p in terms of S. For simplicity, correlations were sought predicting each property in terms of only one other property instead of a combination of other properties. Also, since plots of each and every pair of properties demonstrated that, in all cases, where a relationship existed it was approximately linear, only linear correlations were considered. In developing such correlations, the method of least squares was used. The correlations developed are given by the following equations:

$$\rho_T = 4.489 - 0.664 d_c \qquad \overline{R} = 0.01 \qquad (1)$$

$$V_p = \begin{cases} -0.1066 + 0.00924\epsilon & \overline{R} = 10.6 \quad (2) \\ -0.00142 + 0.00654\theta_{air} & \overline{R} = 7.6 \quad (3) \\ 0.7970 - 0.3980\rho_p & \overline{R} = 11.1 \quad (4) \end{cases}$$

$$v_p = -0.0046 + 0.00295S \qquad \overline{R} = 12.5 \qquad (5)$$

$$A_p = \begin{cases} 0.072 + 0.846S & \overline{R} = 4.7 \quad (6) \\ 0.37 + 238.0 v_p & \overline{R} = 10.8 \quad (7) \end{cases}$$

$$r_a = 0.2 + 2.21 r_m \qquad \overline{R} = 4.2 \qquad (8)$$

$$\epsilon = \begin{cases} 12.10 + 0.670\theta_{air} & \overline{R} = 3.8 \quad (9) \\ 10.41 + 0.710\theta_{Hg} & \overline{R} = 5.7 \quad (10) \\ 98.29 - 43.36\rho_P & \overline{R} = 0.8 \quad (11) \end{cases}$$

$$\theta_{air} = 120.68 - 60.01\rho_P \qquad \overline{R} = 7.2 \qquad (12)$$

$$\theta_{Hg} = \begin{cases} 110.43 - 53.15\rho_P & \overline{R} = 10.2 \quad (13) \\ 3.49 + 0.889\theta_{air} & \overline{R} = 6.6 \quad (14) \\ 3.71 + 135.7V_p & \overline{R} = 2.2 \quad (15) \end{cases}$$

Predicted values from these correlations are compared with measured values in figure 4. All correlations have a correlation coefficient greater than 0.92 except the correlation of pore area in terms of pore volume which has a correlation coefficient of 0.89.

It is pointed out that a correlation was developed relating ρ_T to d_c (eq. (1)) even though ρ_T is defined in terms of d_c because such a linear expression might be desirable for some purposes; the remaining correlations were developed for pairs of variables having no previously known functional relationship. It is noted that four material properties (V_p, A_p, ϵ, and θ_{Hg}) can be correlated satisfactorily by two or more expressions. It is also interesting to note that of the eight material properties correlated, four (V_p, ϵ, θ_{air}, and θ_{Hg}) can be correlated satisfactorily in terms of the bulk density ρ_P. It is not surprising, then, that bulk density should have become a most important property in selecting graphites for consideration as ablators.

Since two variables are obviously not independent if one can be predicted from the other, the total number of properties under consideration for describing the various artificial graphites can be reduced by using the correlations shown in equations (1) to (15). Hence it is seen that out of the original 18 material properties only the 10 properties ρ_P, ρ_{air}, R_p, G_m, S, r_m, r_p, $\overline{A}$, d_c, and k are truly independent. This reduction in material properties requiring consideration represents a savings in both experimental and computational time.

Treatment of Ablation-Performance Data

In order to determine which of these 10 material properties have the most pronounced effect on graphite ablation performance in the present test environment, attempts were made to relate the five ablation-performance parameters Δl, T, $\dot{s}$, τ, and Γ

(considered as dependent variables) to the 10 material properties (considered as independent variables). Standard methods of stepwise multiple, curvilinear regression were used (ref. 15). Each material property was considered in the regression equation to the first power alone, and to both the first and second power according to the general expression $y = c + \sum_{i=1}^{10}\left(a_i x_i + b_i x_i^2\right)$, where y represents an ablation performance parameter, x_i the i^{th} material property being considered, and a_i, b_i, and c the coefficients calculated from the regression. Although this form of equation obviously cannot yield information regarding a true functional relationship or mechanism, it can identify those variables which are functionally related in a statistical sense, and, furthermore, can indicate the direction of the functional dependence – that is, whether an increase (or decrease) in the value of a certain material property will result in an increase or decrease in the value of an ablation parameter of interest. The main purpose in formulating the regression equations was not to determine a true functional mechanism nor to predict ablation performance (though it can, in some cases, be useful for this), but was to identify those material-property variables which have the strongest effect on ablation performance.

Since the computations required are extensive, all computations were performed on a digital computer using a modified form of a computer program written by Efroymson (ref. 16). One very useful feature of this computer program is that it automatically tests against a preselected significance level the significance for entry of each of the x_i and x_i^2 into the regression equation. This insures that all of the x_i and x_i^2 in the final regression equation are statistically significant at the preselected level. Accordingly, all variables having only a random effect (at the selected significance level) are automatically excluded. The computer program used is given in appendix C.

RESULTS AND DISCUSSION

Dependence of Ablation Performance on Material Properties

Regression equations for the five ablation parameters were formulated in terms of the 10 independent property variables at a significance level of 1 percent. A 1-percent significance level means that if a given property appears in the final regression equation, there is only a 1-percent statistical probability of its having been erroneously included, or, in other words, there is only one chance in 100 of that variable having but a random effect on the dependent variable (i.e., on the ablation parameter). It is important to recognize, however, that such a significance criterion does not guarantee that every variable which has a true effect on ablation performance has been discovered; neither does it absolutely guarantee that every variable which is singled out by the significance test as having an effect does, in fact, have such an effect. What it does guarantee is that, for

each of those variables singled out, there is only one chance in 100 (1-percent statistical probability) of that variable not having a real effect.

Obviously a significance level other than the present 1-percent level could have been chosen; the precise choice must be made on the basis of the degree of risk one is willing to take in incorrectly assuming that a variable has an effect when it really does not. The reasoning behind the present choice of 1 percent was that if a graphite manufacturer were to attempt to fabricate an improved graphite by accepting the property variables singled out by the regression equations as important, and were to proceed by adjusting his formulation and fabrication techniques to optimize these variables, he might reasonably desire the assurance that there be only one chance in 100 that he is proceeding in an unprofitable direction. A matter of some interest, however, is that even though the present regression equations were formulated at a significance level of 1 percent, it turns out that all variables are also significant at the 0.5-percent level. In other words, if one accepts the singled-out property variables as being important, there is actually only one change in 200 of his being wrong.

Regression equations were formulated for all five ablation parameters considering the material-property variables to the first power only, and also to both the first and second powers. In both cases, the material properties singled out as significant were identical; therefore, only those regression equations obtained by considering the material-property variables to the first power alone are presented. The resulting regression equations, with their average absolute percent residuals $\overline{R}$, are given by

$$\Delta l = 2.073 - 0.985\rho_p + 0.437G_m \qquad \overline{R} = 12.3 \qquad (16)$$

$$T = 2169.9 + 157.8G_m + 0.0201\overline{A} - 67.4k \qquad \overline{R} = 1.5 \qquad (17)$$

$$\dot{s} = 0.05156 - 0.02145\rho_p + 0.01596G_m \qquad \overline{R} = 10.7 \qquad (18)$$

$$\tau = 0.7 + 2.7G_m \qquad \overline{R} = 14.9 \qquad (19)$$

$$\Gamma = 6.2 - 3.1\rho_p + 2.5G_m \qquad \overline{R} = 28.0 \qquad (20)$$

Equations (16) to (20) clearly reveal the importance of maximum grain size G_m and bulk density ρ_p in determining ablation performance. Maximum grain size is the only property appearing in all five regression equations. As G_m increases, so do Δl, T, $\dot{s}$, τ, and Γ. This result is in agreement with the currently accepted practice of selecting fine-grained graphites for ablation materials. Equation (19) indicates that surface texture τ is a function of G_m only, which certainly appears reasonable. That Δl and $\dot{s}$ are strongly dependent on G_m (see eqs. (16) and (18)) could imply, among other things, a contribution of particle removal to the ablation process (ref. 17). Bulk density ρ_p also affects Δl and $\dot{s}$, with equations (16) and (18) indicating that an

increase in ρ_p produces a corresponding decrease in $\Delta\ell$ and $\dot{s}$. This is most reasonable because for a given rate of reaction (rate of removal of mass) dimensional changes will be smaller the denser the graphite. This predicted behavior of higher densities resulting in smaller values of $\Delta\ell$ and $\dot{s}$ is consistent with current practice of selecting high-density graphites for ablation applications. Also, as seen from equation (20), higher densities tend to reduce the degree of gouging of an ablating graphite.

Ash content $\overline{A}$ is seen from equation (17) to affect surface temperature T, with higher values of $\overline{A}$ resulting in higher surface temperatures. This result is to be expected, since the presence of chemical impurities in an artificial graphite is known to catalytically accelerate its oxidation rate (refs. 1 and 2), driving the surface temperature higher by the exothermicity of the reaction. A reasonable upper limit on ash content can be derived from equation (17). For instance, since an ash content of 100 ppm produces an increase in surface temperature of only about 2 K, it seems reasonable that one might want to maintain the ash content at or below that level, which is not at all difficult to achieve. It is also seen from equation (17) that thermal conductivity k has a negative effect on surface temperature. This result, again, is most reasonable since higher values of k will serve to increase the rate of heat transfer from the stagnation point to the sides and other parts of the graphite specimen. Thus, on the whole, it appears that the material properties primarily responsible for determining the ablation performance of a typical artificial graphite are G_m, ρ_p, $\overline{A}$, and k.

Since artificial graphites which develop roughened surfaces or become gouged during ablation are often undesirable in practical applications, criteria by which such graphites can be eliminated from consideration are valuable. Equations (19) and (20) provide such criteria. For instance, if graphite surface texture is required to be $\tau \leqq 1.3$, application of equation (19) shows that all those graphites with grain sizes $G_m > 0.22$ mm should be eliminated. Examination of table I shows that there are 11 graphites of the first 40 having $G_m > 0.22$ mm. Of these 11, only two had smooth surfaces after testing; at the same time, only one graphite (4007) would not be eliminated which had a slightly roughened surface ($\tau = 2$). Now, in addition, if it is also required that the degree of gouging be $\Gamma \leqq 1.5$, application of equation (20) indicates that additional graphites should be eliminated. Since Γ is a function of both density ρ_p and maximum grain size G_m, the criteria for elimination of graphites will be in terms of both variables. The simplest way to establish these criteria is to calculate, for each different value of maximum grain size, that value of density below which if the actual graphite density falls, the graphite is to be eliminated. A list of such density values for the 11 different values of maximum grain size of the present graphites is shown in table III. In addition to the 11 graphites already eliminated by the requirement that $\tau \leqq 1.3$ ($G_m \leqq 0.22$ mm), eight more will be eliminated by the added requirement that $\Gamma \leqq 1.5$ (given by the criteria in table III). The one graphite (4007) not eliminated previously which had a slightly roughened surface is

now eliminated by this additional requirement. Note also that this graphite is severely gouged ($\Gamma = 3$). Considered by itself, the requirement that $\Gamma \leq 1.5$ eliminates all but one graphite which should be eliminated (H205-85 with $\Gamma = 2$), and eliminates only three graphites which were, in fact, not gouged.

Elimination of the 19 graphites indicated by these two requirements on surface texture and degree of gouging produces a subset of the original data set which is comprised of graphites virtually all of which erode with smooth, ungouged surfaces. This subset may then be analyzed in a manner similar to that of the original data set – that is, regression equations can be formulated for the ablation parameters $\Delta\ell$, T, and $\dot{s}$, in terms of the 10 material properties. This was done, as before, at the 1-percent significance level, with the results that $\Delta\ell$ is solely a function of ρ_p, that T is a function of r_m and $\overline{A}$, and that $\dot{s}$ does not correlate with any material property. However, because the reduced number of data sets for this analysis (21 as opposed to the original 40) makes it more likely that the high significance level (1 percent) will cause important variables to be omitted from the regression equations, this significance level was relaxed somewhat to the 2.5-percent level (the next lower significance level at which statistical tests are customarily made). At this 2.5-percent level, the following regression equations were obtained:

$$\Delta\ell = 1.587 - 0.583\rho_p + 1.82 \times 10^{-5}\overline{A} - 2.97 \times 10^{-3} r_m \qquad \overline{R} = 4.7 \qquad (21)$$

$$T = 2843.1 - 5.475 r_m + 0.0294\overline{A} - 253.4\rho_p \qquad \overline{R} = 1.0 \qquad (22)$$

$$\dot{s} = 0.03457 - 0.01028\rho_p \qquad \overline{R} = 5.5 \qquad (23)$$

Bulk density ρ_p is seen to affect $\Delta\ell$ and $\dot{s}$ as before; that is, the greater the density, the smaller $\Delta\ell$ and $\dot{s}$. Density is also seen to influence T, with lower values of T the higher the density. Also as before, an increase in ash content $\overline{A}$ is seen to produce a higher surface temperature; but $\overline{A}$ is also indicated as having an effect on $\Delta\ell$ (higher $\overline{A}$ producing larger $\Delta\ell$). This is, of course, again consistent with the known effects of chemical impurities catalytically accelerating oxidation rate (refs. 1 and 2). The reason why $\overline{A}$ is not also indicated as having an effect on $\dot{s}$ is very likely associated with the fact that $\dot{s}$, being a much more difficult parameter to measure than $\Delta\ell$, is known less accurately, and as the error in a dependent variable increases, the sensitivity of the regression analysis decreases. In fact, it so happens that if the significance level criterion is relaxed to about the 7.5-percent level, $\overline{A}$ is the next property variable to enter the regression equation for $\dot{s}$, and, as should be the case, an increase in $\dot{s}$ is predicted by an increase in $\overline{A}$. The influence of r_m on $\Delta\ell$ and T is interesting and bears further investigation. However, it is gratifyingly assuring that a change in r_m causes both $\Delta\ell$ and T to change in the same direction, since a change in opposite

directions for Δl and T is most unlikely. Hence, taken together, equations (21) to (23) reveal that ρ_p, $\overline{A}$, and r_m are the material properties of importance in determining the ablation performance of a typical artificial graphite intentionally selected to ablate with a smooth, ungouged surface.

In addition to the previously discussed theoretical limitations concerning regression equations in general, there are other possible, more practical limitations on the present regression equations (eqs. (16) to (23)). Primary among these is the possibility that not all of the important material properties may have been included in the list of properties considered. Several potentially important properties not included are: the raw materials, filler-to-binder ratio, grain-size distribution (instead of merely the maximum grain size), the distribution of impurities between filler and binder carbons, the lattice dimensions of the binder, the nature of the bonding between the filler and binder, the type of porosity, the gas permeability, tensile strength, shear strength, Young's modulus, etc. Some of this information is difficult or, in the case of proprietary information, impossible to obtain. Even if all this information were available, some is difficult to specify quantitatively in meaningful terms (for instance, the distribution of impurities between filler and binder carbons). But, in spite of the possible omission of some potentially important material properties, the present analysis has revealed five material properties to be important in determining ablation performance $(G_m, \rho_p, \overline{A}, k, \text{and } r_m)$. Of particular importance, also, is that the present method of analysis has been shown to be both powerful and efficient, at no time contradicting either experience or reason in predicting a given material property to be important or in predicting the direction of the effect which a given material property has on ablation performance.

The information gained from the regression equations in this study should be useful in selecting artificial graphites for consideration for use in environments similar to that of the present test environment, and also as a guide to future research. Certainly the present method of analysis appears particularly effective. For a more complete picture of the various material properties affecting graphite ablation performance, it would be desirable to apply the present approach to ablation data obtained in different environments spanning a wide range of pressures and enthalpies. Similar regression equations could be developed for these different environments and, as in the present study, criteria could be established for the elimination of those graphites which are likely to develop undesirably rough surface, unacceptably high degrees of gouging, or other undesirable characteristics. A more fundamental investigation could perhaps be conducted by carefully controlling the fabrication of different graphites, with each graphite differing systematically in its material properties. The severe difficulty to be encountered in this approach, however, is that it is almost impossible to alter the value of any one material property without at the same time altering many others as well. A combination of these two

approaches – controlled fabrication and statistical treatment of the data – may well be the most promising approach for future work.

Comparisons With Previous Work

Several other investigations also attempting to determine the effect of material properties on the erosion behavior of graphite in high temperature dynamic environments have been reported (refs. 18 to 20). Slosarik and Swope (ref. 18) and Chase (ref. 19) investigated the effects of certain material properties on rocket-nozzle erosion and McVey, Auerbach, and McBride (ref. 20) investigated material-property effects on ablation. Slosarik and Swope considered the properties of density, porosity, pore-size distribution, tensile strength, and impurity content, but could find no direct, unambiguous effects. However, they concluded from the trends of their data that high density, low porosity, low impurity content, high tensile strength, and a small number of larger sized pores are important for good erosion resistance. Chase (ref. 19) considered flexural strength, density, and porosity and concluded that all three "play their part in determining erosion resistance." McVey, Auerbach, and McBride (ref. 20) considered the effect of graphite microstructure on ablation performance, and concluded that grain size, filler-to-binder ratio, porosity, porosity type, grain orientation, and degree of graphitization all affect ablation performance.

All three of these reported investigations suffer from the weakness that in attempting to determine which material properties most strongly affect ablation performance, each material property was considered separately, one by one, for its individual effect on ablation performance. In many cases, the data presented are ambiguous and open to several different interpretations. Consequently, many of the conclusions reached, though sufficiently reasonable, are actually based on theoretical or intuitive arguments and lack the necessary supporting experimental data. Two of the conclusions reached by McVey, Auerbach, and McBride (ref. 20), however, conflict with results obtained in the present study or with those of other studies. These conclusions are that grain orientation is important, and that the greater the degree of graphitization, the more readily the graphite will ablate. In conflict with their first conclusion are the experimental results of reference 2 demonstrating that grain orientation has little effect on the ablation performance of artificial graphite. Conflicting with their second conclusion is the discussion in reference 3 which points out that the oxidation rate of a graphite should, if anything, decrease with increasing degree of graphitization. Furthermore, since degree of graphitization is directly related to interlayer spacing d_c (ref. 3) which does not appear in the regression equations of the present study, it would appear that degree of graphitization is not one of the more important material properties affecting ablation performance. One possible explanation why McVey, Auerbach, and McBride arrived at these two debatable conclusions is that they studied an extremely broad diversity of carbonaceous materials –

commercial graphite, a carbon felt impregnated with pyrolytic carbon, and a composite material consisting of carbon fibers in a graphitized matrix – as opposed to studying a single class of carbonaceous materials such as commercial artificial graphite, for instance. For the materials they studied, the precise significance of a number of the material properties is vague. Certainly the conventional concept of grain orientation, and perhaps even degree of graphitization lose much of their significance.

It is of some interest to note that all three investigations cited above (refs. 18 to 20) report porosity to be an important variable, with the first two investigations also reporting density to be important. This is not surprising considering that it has been shown in the present study that total porosity ϵ can be predicted in terms of bulk density ρ_p to less than 1 percent and open porosity (θ_{air} and θ_{Hg}) can be predicted to within 10 percent or less (eqs. (11) to (13)). Hence, the conclusion that porosity is important is merely an alternative way of stating that density is important. The two conclusions should therefore not be considered as separate – at least, not until a separation can be made on the fundamental basis of mechanism.

Predictions of Ablation Performance of Several Graphites

As mentioned previously, several graphites were added during the experimental program and complete material-property data were not determined on them. These graphites, the last five in table I, were included in the investigation because of special characteristics of possible value: AGOT graphite was chosen because it is reported to be unusually resistant to the propagation of cracks caused by thermal shocking (ref. 21); AXF-5Q graphite was chosen because of its exceedingly fine grain size; and the three Graph-i-tite graphites were chosen because of reports (unpublished) of high erosion resistance in ablation tests. Also as mentioned previously, since the property data on these graphites are incomplete, they were not included in the development of the regression equations (eqs. (16) to (23)). Nonetheless, some property data are available on these graphites (table I), and even though the expressed purpose in developing the present regression equations was simply to isolate those material properties having the strongest effect on ablation performance, it is possible to predict ablation performance for some of these graphites and to compare this predicted performance with actual measurements.

Ablation-performance predictions can be made for AGOT, AXF-5Q, Graph-i-tite "A," and the Graph-i-tite "G" graphite which has a maximum grain size of 0.840 mm. (The Graph-i-tite "G" graphite with a maximum grain size of 0.203 mm was tested in a different series of tests at a somewhat higher heating rate than the other graphites (562 W/cm^2) and therefore predictions of ablation performance are not strictly comparable.) Ablation performance predictions have been made using equations (16) to (20), where appropriate, with the results shown in table IV. The only acceptable agreement between predicted and

measured ablation performance is for surface texture τ and degree of gouging Γ. Agreement for surface temperature T is not bad; but, then, since the spread in test temperatures is not large, the predicted temperatures cannot be too far off. For Δl and $\dot{s}$, the predicted values for the large-grained graphites are too large and the predicted value for the small-grained graphite is too small. This lack of agreement is possibly related to the special nature of these graphites, with the direction of the discrepancy undoubtedly being due to the strong dependence of Δl and $\dot{s}$ on G_m.

The application of the criteria established by the requirements on surface texture and degree of gouging discussed previously ($\tau \leqq 1.3$ and $\Gamma \leqq 1.5$) would eliminate AGOT, Graph-i-tite "A," and the large grained form of Graph-i-tite "G" from consideration. This is as it should be, since these graphites developed roughened, gouged surfaces during ablation. The remaining two graphites (AXF-5Q and the fine grained form of Graph-i-tite "G") both have smooth, ungouged surfaces. Equations (21) to (23), then, ought to be appropriate for predicting their ablation performance. This can be done only for AXF-5Q, however, because, as previously stated, these equations are not strictly applicable to this fine-grained form of Graph-i-tite "G" since it was ablation tested at a heating rate different from that at which the regression equations were formulated. In attempting these predictions, it is noted that mean pore radius r_m appears in the equations for both Δl and T, and since r_m is not known for AXF-5Q, Δl and T cannot be calculated. However, $\dot{s}$ is a function of ρ_p alone (eq. (23)) and, therefore, values of $\dot{s}$ can be calculated. Its predicted value, given in table IV, is seen to be lower than the experimental value, but not as low as that predicted by equation (18), which includes a term for the maximum grain size. It is worth reemphasizing, however, that the main value of the present regression equations is in identifying the important material properties and the directions in which they affect ablation performance, and not in predicting ablation performance itself.

CONCLUSIONS

Measurements of 18 material properties and of ablation performance in one test environment have been made on 45 commercial, artificial graphites. As a result of these measurements and an analysis of the data, the following conclusions and recommendations are drawn.

1. Correlations between pairs of the 18 graphite material properties have been developed where possible, thus enabling certain properties to be predicted in terms of others. The original 18 material properties were thereby reduced to 10 mutually independent properties.

2. A correlation based on 10 selected graphites was developed relating thermal conductivity to electrical conductivity. This correlation is in good agreement with

existing correlations in the literature, but was formulated specifically for the present graphites which have thermal and electrical conductivities extending to lower values than had been included in previous correlations of thermal and electrical conductivity.

3. Regression equations have been developed at the 1-percent significance level relating the ablation performance of artificial graphite in the present test environment (Mach 2 airstream, stagnation pressure of 5.6 atm, and enthalpy of 2.2 MJ/kg) to graphite material properties. These regression equations which, in fact, are even significant at the 0.5-percent level, demonstrate that ablation performance depends on maximum grain size, bulk density, ash content, and thermal conductivity.

4. Criteria have been established from these regression equations for eliminating those graphites likely to develop rough surfaces or become gouged during ablation. After elimination of these graphites, a second set of regression equations have been developed relating ablation performance to material properties. These equations reveal that ablation performance of artificial graphites intentionally selected to ablate with smooth, ungouged surfaces depends on bulk density, ash content, and mean pore radius.

5. Maximum grain size is an important property in determining ablation performance, with an increase in maximum grain size causing an increase in total length change, surface temperature, recession rate, surface texture, and degree of gouging. To ensure a smooth surface, maximum grain size should be kept below 0.22 mm.

6. Bulk density is also of prime importance in determining ablation performance, with higher densities resulting in lower values of total length change, recession rate, and degree of gouging.

7. High ash content produces higher surface temperatures, while high values of thermal conductivity and mean pore radius tend to produce lower surface temperatures.

8. In spite of certain theoretical and practical limitations, the present method of analysis (stepwise multiple regression) for identifying the more important graphite material properties affecting ablation performance is both powerful and efficient. Its soundness is demonstrated by the fact that it properly predicts ablation performance to be related to certain material properties known from theoretical or experimental considerations to affect ablation performance.

9. In order to determine other material properties which might also have an important effect on ablation performance, a more extensive list of properties than the 18 considered here could be employed. Also, testing should be conducted in a wider range of environments. A desirable addition to such a study would be the systematic, controlled fabrication of different graphites, differing, insofar as possible, in only one property at a time.

10. Graph-i-tite "G" graphite is particularly erosion resistant, even more so than the usual standard of comparison, ATJ graphite. Whereas the larger-grained Graph-i-tite "G" (maximum grain size of 0.840 mm) became rough during ablation, the finer-grained Graph-i-tite "G" (maximum grain size of 0.203 mm) remained smooth, thus making it particularly attractive for future study.

Langley Research Center,
National Aeronautics and Space Administration,
Hampton, Va., January 7, 1972.

APPENDIX A

PREDICTIONS OF THERMAL CONDUCTIVITY FROM ELECTRICAL CONDUCTIVITY

Reference 9 reports the relation $k = 1.297 \times 10^{-3} \sigma_E$ for predicting thermal conductivity from electrical conductivity (at room temperature). In order to verify this relation for the present graphites, both thermal conductivity and electrical conductivity were experimentally measured on 10 of the graphites. These 10 graphites were selected from the total number of graphites in the present study to span the full range of measured electrical conductivities in approximately equal increments. Thermal-conductivity measurements were made using a comparative longitudinal heat-flow apparatus and were performed by the Oak Ridge National Laboratory on the same samples used for the electrical-conductivity measurements. This apparatus consists of a vacuum chamber containing an axial column of two instrumented Armco iron heat meter bars between which the specimen is compressed. A heater on one of the meter bars induces heat flow in the column and axial temperature distributions are measured with thermocouples on the bars.

The resulting thermal and electrical-conductivity data are plotted in figure 5, with the curve through the data being given by the expression

$$k = 1.513 \times 10^{-3} \sigma_E - 0.1388 \times 10^{-6} \sigma_E^2$$

This equation was developed from the data by the method of curvilinear least squares. It was formulated specifically for the present graphites because they include thermal and electrical conductivities extending to lower values than had been included in previous correlations of thermal and electrical conductivity. Predictions of thermal conductivity from this equation compare favorably with predictions from the equation of reference 9, and even more favorably with predictions from an equation developed by the Oak Ridge National Laboratory

$$k = 1.56 \times 10^{-3} \sigma_E - 0.266 \times 10^{-6} \sigma_E^2$$

This latter equation was developed from more extensive data, including data on the 10 NASA graphites, as well as on other graphites with electrical conductivities extending as high as 1940 $(\Omega\text{-cm})^{-1}$.

APPENDIX B

ABLATION PERFORMANCE OF Graph-i-tite "G"

During the course of the present investigation it was observed that the Graph-i-tite "G" graphite being tested (maximum grain size 0.840 mm) was particularly more erosion resistant than the other graphites under test. However, anomalously, it also eroded to produce a very rough surface. It was reasoned that its rough surface must be due to its large grain size, but that its high erosion resistance must be due to other factors. Since Graph-i-tite "G" is also available with the smaller maximum grain size of 0.203 mm, it was further reasoned that this fine-grained form might be as erosion resistant as the large-grained form, but at the same time erode with a smooth surface. Accordingly, some of the fine-grained material was obtained, and a brief test series conducted in which the ablation performances of Graph-i-tite "G" (G_m = 0.840 mm), Graph-i-tite "G" (G_m = 0.203 mm), and ATJ were compared. (The ATJ was selected because it is a commonly used standard of comparison.) Nominal heating rate (562 W/cm^2) was somewhat higher in these tests than in the others.

Results of this test are shown in table II, where it is observed that, within experimental scatter of the test, the recession rates $\dot{s}$ of the two Graph-i-tite "G" graphites are virtually identical, but significantly lower than that of ATJ. Also, the total recessions $\Delta\ell$ of the two Graph-i-tite "G" materials are close, but, again, are much lower than that of ATJ. It appears from these tests, therefore, that the fine-grained form of Graph-i-tite "G," which, in fact, did erode with a smooth, ungouged surface (see table I), may offer improved ablation performance compared with that of other graphites currently in use.

APPENDIX C

COMPUTER PROGRAM FOR STEPWISE MULTIPLE CURVILINEAR REGRESSION

The computer program used is a modified form of that written by Efroymson (ref. 16). The computational procedure is the same as that originally written by Efroymson, but a number of options have been added to the program making it more flexible.

Certain important details of the program are that the number of independent variables is limited to 49, and the number of sets of observations is limited to 100. A weighting factor can be assigned to each set of data if desired. A significance level must be chosen and a corresponding F-level (see, for instance, ref. 15) must be set for the entry of a variable into the regression equation. The computation then considers each independent variable step by step with a variable entering the equation only if it produces a statistically significant reduction in the residual sum of squares about regression (at the chosen F-level).

The data are read in according to the format 6F12.5, with all the independent variables of a set read in first, followed by the dependent variable, and followed, in turn, by the weighting factor, if any. The control card is written as follows:

Col. no.	Variable	Description
1-10	TOL	Tolerance (set at 0.001)
11-20	EFIN	F-level to enter variables into regression
21-30	EFOUT	F-level to remove variables
31-35	NOPROB	Problem number
36-40	INVAR	1 greater than the number of independent variables read in as data
41-45	NODATA	Number of data sets
48	IFWT	1, if no weighting factors assigned
50	IFSTEP	1, if intermediate steps not to be printed
52	IFRAW	1, if residual sums and squares not to be printed
54	IFAVE	1, if average not to be printed
56	IFRESD	1, if residual squares and cross products not to be printed
58	IFCOEN	1, if partial correlations not to be printed
60	IFPRED	1, if predicted values not to be printed
62	IFCNST	1, if constant term in regression equation is assumed to be zero
64	IFDATA	1, if input data not to be printed

Col. no.	Variable	Description
66	IFPWR	1, if second power of variables not to be considered
68	IFPLOT	1, if predicted values not to be plotted against measured values

The F-level is based on 1 and (NODATA - NOVAR) degrees of freedom where NODATA is the number of data sets and NOVAR is 1 greater than the total number of independent variables considered in the regression equation. (In the case where the second power of the variables is to be considered, the number of independent variables considered in the regression equation is obviously twice the number of variables appearing as raw data.) The F-level for entering variables must be greater than or equal to the F-level for removing variables. A complete listing of the computer program is given below.

```
C       SIMPLE STEPWISE MULTIPLE-CURVILINEAR REGRESSION
C       CONSIDERS EACH VARIABLE TO 1ST POWER, 2ND POWER IF DESIRED
        DIMENSION DATA(50),VECTOR(50,50),AVE(50),SIGMA(50),
       1COEN(50),SIGMCO(50),INDEX(50),DATAS(100,50),X(100),Y(100)
        DIMENSION IN(2)
C       INVAR = 1 + NO. OF INDEPENDENT VARIABLES READ IN AS DATA
C       NOVAR = 1 + TOTAL NO. OF INDEPENDENT VARIABLES CONSIDERED BY PROGRAM
C       NODATA = NO. OF DATA SETS
C       FFIN AND FFOUT ARE BASED ON 1 AND (NODATA - NOVAR) DEGREES OF FREEDOM
  100   READ (5,5) TOL,FFIN,FFOUT,NOPROB,INVAR,NODATA,
       1IFWT,IFSTEP,IFRAW,IFAVE,IFRESD,IFCOEN,IFPRED,IFCNST,IFDATA,IFPWR,
       2IFPLOT
        IF (EOF,5) 998,999
  998   STOP
  999   CONTINUE
C       IFWT=1,THEN WHTS=1.0
C       IFSTEP=1,DO NOT PRINT EACH STEP
C       IFRAW= 1,DO NOT PRINT RAW SUMS AND SQUARES
C       IFAVE= 1,DO NOT PRINT AVERAGES
C       IFRESD=1,DO NOT PRINT RESIDUAL SUMS SQUARES
C       IFCOEN=1,DO NOT PRINT PARTIAL COEFFICIENTS
C       IFPRED=1,DO NOT CALC  PREDICTED VALUES
C       IFCNST=1,DO NOT HAVE  CONST TERM IN EQUATION
C       IFDATA=1,DO NOT PRINT INPUT DATA
C       IFPWR=1, DO NOT CONSIDER VARIABLES TO 2ND POWER
C       IFPLOT=1, DO NOT PLOT DATA
        ITAPE=6LTAPE99
        IN(1)=10H1232  HGMH
        DIV=3HAMP
        PROB=4H PRB
        YAX=6HY CALC
        XAX=6HY DATA
        INVARMI=INVAR-1
        NOIN=0
        VAR=0.
        K    =0
        FLEVEL=0.
        NOENT=0
        NOMIN=0
        NOMAX=0
```

```
      RNODATA=NODATA
      S1=0.
      S2=0.
      S3=0.
      S4=0.
      IF(IEPWR) 900,410,412
  410 NOVAR=2*(INVAR-1)+1
      NVP1=NOVAR+1
      NIX=1
      IF(NOVAR-50) 110,110,1801
  412 NOVAR=INVAR
      NVP1=NOVAR+1
      NIX=1
    2 IF(INVAR-50) 110,110,1800
  110 DO 120 I=1,NVP1
  130 DO 120 J=1,NVP1
  120 VECTOR(I,J)=0.0
  140 IF (IEWT) 900,500,150
  900 WRITE (6,905)
      GO TO 910
  150 DO 170 N=1,NODATA
C....READ INPUT DATA (W/O WEIGHTS), FORMAT 10
      READ(5,10) (DATA(L),L=1,INVAR)
      IF(IEPWR) 900,414,418
  414 DATA(NOVAR)=DATA(INVAR)
      DO 416 L=1,INVARMI
      KK=INVARMI+L
  416 DATA(KK)=DATA(L)**2
  418 DO 181 L=1,NOVAR
  181 DATAS(N,L)=DATA(L)
  180 DO 190 I=1,NOVAR
  200 VECTOR(I,NOVAR+1)=VECTOR(I,NOVAR+1)+DATA(I)
  210 DO 220  J=I,NOVAR
  220 VECTOR(I,J)=VECTOR(I,J)+DATA(I)*DATA(J)
  190 CONTINUE
  170 VECTOR(NVP1,NVP1)=VECTOR(NVP1,NVP1)+1.0
  230 GO TO 565
C     CALCULATION SUMS WHEN VARIABLE WEIGHTS
  500 DO 510 N=1,NODATA
C....READ INPUT DATA (W, WEIGHTS), FORMAT 10
      READ(5,10) (DATA(L),L=1,INVAR),WHT
      IF(IEPWR) 900,420,424
  420 DATA(NOVAR)=DATA(INVAR)
      INVARMI=INVAR-1
      DO 422 L=1,INVARMI
      KK=INVARMI+L
  422 DATA(KK)=DATA(L)**2
  424 DO 182 L=1,NOVAR
  182 DATAS(N,L)=DATA(L)
  530 DO 540 I=1,NOVAR
  550 VECTOR(I,NOVAR+1)=VECTOR(I,NOVAR+1)+DATA(I)*WHT
  560 DO 540 J=I,NOVAR
  540 VECTOR(I,J)=VECTOR(I,J)+DATA(I)*DATA(J)*WHT
  510 VECTOR(NVP1,NVP1)=VECTOR(NVP1,NVP1)+WHT
C     COMPLETED SUMS OF SQUARES AND CROSS PRODUCTS. THESE ARE IN
C     STORAGE IN LOCATION,VECTOR(I,J). THESE WILL BE PRINTED OUT ON
C     TAPE 6 UNDER CONTROL OF STATEMENT 100
```

```
  565 CONTINUE
      NOVMI=NOVAR-1
  566 NOVPL=NOVAR+1
  567 WRITE (6,90) NOPROB,NODATA,NOVAR,VECTOR(NOVPL,
     1NOVPL),EFIN,EFOUT
      IF(IFDATA) 900,400,570
  400 WRITE (6,9)
      DO 183 N=1,NODATA
C....WRITE INPUT DATA, FORMAT 12
  183 WRITE(6,12) (DATAS(N,L),L=1,INVARMI), DATAS(N,NOVAR)
      WRITE(6,11)
  570 IF (IFRAW) 900,580,650
  580 WRITE (6,15)
  590 WRITE (6,20) (I,VECTOR(I,NOVPL),I=1,NOVMI)
  600 WRITE (6,25) VECTOR(NOVAR,NOVPL)
  610 WRITE (6,30)
  620 WRITE (6,35) ((I,J,VECTOR(I,J),J=I,NOVMI),I=1,NOVMI)
  630 WRITE (6,40) (I,VECTOR(I,NOVAR),I=1,NOVMI)
  640 WRITE (6,45) VECTOR(NOVAR,NOVAR)
      GO TO 650
C     CALCULATION OF RESIDUAL SUMS OF SQUARES AND CROSS PRODUCTS
  650 IF (IFCNST) 900,651,735
  651 IF (VECTOR(NOVPL,NOVPL)) 652,652,655
  652 WRITE (6,654)
      GO TO 910
  655 DO 660  I=1,NOVAR
  670 DO 660  J=I,NOVAR
  660 VECTOR(I,J)=VECTOR(I,J)-(VECTOR(I,NOVPL)*VECTOR(J,NOVPL)
     1/VECTOR(NOVPL,NOVPL))
  680 DO 690 I=1,NOVAR
  690 AVE(I)=VECTOR(I,NOVPL)/VECTOR(NOVPL,NOVPL)
  700 IF (IFAVE) 900,710,735
  710 WRITE (6,50)
  720 WRITE (6,20) (I,AVE(I),I=1,NOVMI)
  730 WRITE (6,25) AVE(NOVAR)
  735 IF (IFRESD) 900,740,780
  740 WRITE (6,55)
  750 WRITE (6,35)((I,J,VECTOR(I,J),J=I,NOVMI),I=1,NOVMI)
  760 WRITE (6,40) (I,VECTOR(I,NOVAR),I=1,NOVMI)
  770 WRITE (6,45) VECTOR(NOVAR,NOVAR)
  780 NOSTEP=-1
  781 ASSIGN 1320 TO NUMBER
  782 DEFR=VECTOR(NOVPL,NOVPL)-1.0
  790 DO 800  I=1,NOVAR
  791 IF (VECTOR(I,I)) 792,794,810
  792 WRITE (6,793) I
      GO TO 910
  793 FORMAT (31H ERROR RESIDUAL SQUARE VARIABLE I4,31H IS NEGATIVE,PROB
     1LEM TERMINATED)
  794 WRITE (6,795) I
  796 SIGMA(I)=1.0
  797 GO TO 800
  795 FORMAT (1H010H VARIABLE I5,13H IS CONSTANT)
  810 SIGMA(I)=SQRT(VECTOR(I,I))
  800 VECTOR(I,I)= 1.0
  820 DO 830 I=1,NOVMI
  840 IP1=I+1
  841 DO 830 J=IP1,NOVAR
  850 VECTOR(I,J)=VECTOR(I,J)/(SIGMA(I)*SIGMA(J))
```

```
  830 VECTOR(J,I)=VECTOR(I,J)
  860 IF (IECOEN) 900,870,1000
  870 WRITE (6,60)
  874 NOVM2=NOVMI-1
  875 DO 885 I=1,NOVM2
  880 IP1=I+1
  885 WRITE (6,35)(I,J,VECTOR(I,J),J=IP1,NOVMI)
  890 WRITE (6,40)(I,VECTOR(I,NOVAR),I=1,NOVMI)
 1000 NOSTEP=NOSTEP+1
 1001 IF (VECTOR(NOVAR,NOVAR)) 1002,1002,1010
 1002 NSTPM1=NOSTEP-1
      WRITE (6,1004) NSTPM1
      GO TO 1381
 1010 SIGY=SIGMA(NOVAR)*SQRT(VECTOR(NOVAR,NOVAR)/DEFR)
 1011 IF (1.0-VECTOR(NOVAR,NOVAR)) 1013,1013,1012
 1012 R=SQRT(1.0-VECTOR(NOVAR,NOVAR))
      GO TO 1015
 1013 R=0.0
 1015 DEFR=DEFR-1.0
 1016 IF (DEFR) 1017,1017,1020
 1017 WRITE (6,1019)  NOSTEP
      GO TO 1381
 1020 VMIN=0.0
 1030 VMAX=0.0
 1035 NOIN=0
 1040 DO 1060  I=1,NOVMI
 1041 IF (VECTOR(I,I)) 1042,1050,1060
 1042 WRITE (6,1044) I,NOSTEP
 1045 GO TO 1381
 1060 IF (VECTOR(I,I)-TOL) 1050,1060,1080
 1080 VAR=VECTOR(I,NOVAR)*VECTOR(NOVAR,I)/VECTOR(I,I)
 1090 IF (VAR) 1100,1050,1110
 1100 NOIN=NOIN+1
 1120 INDEX(NOIN)=I
 1130 COEN(NOIN)=VECTOR(I,NOVAR)*SIGMA(NOVAR)/SIGMA(I)
 1140 SIGMCO(NOIN)=(SIGY/SIGMA(I))*SQRT(VECTOR(I,I))
 1150 IF (VMIN) 1160,1170,904
  904 WRITE (6,906)
      GO TO 910
 1170 VMIN=VAR
 1180 NOMIN=I
 1190 GO TO 1050
 1160 IF (VAR-VMIN) 1050,1050,1170
 1110 IF (VAR-VMAX) 1050,1050,1210
 1210 VMAX=VAR
 1220 NOMAX=I
 1050 CONTINUE
 1230 IF (NOIN) 903,1240,1245
  903 WRITE (6,907)
      GO TO 910
 1240 WRITE (6,65) SIGY
 1260 GO TO 1350
 1245 IF (IECNST) 900,1250,1246
 1246 CNST=0.0
 1247 GO TO 1300
 1250 CNST=AVE(NOVAR)
 1270 DO 1280 I=1,NOIN
 1290 J=INDEX(I)
 1280 CNST=CNST-(COEN(I)*AVE(J))
```

```
1300 IF (IESTEP) 900,1310,1320
1310 IF (NOENT) 1311,1311,1313
1311 WRITE (6,91) NOSTEP,K
1312 GO TO 1314
1313 WRITE (6,92) NOSTEP,K
1314 WRITE (6,70) ELEVEL,SIGY,R,CNST,
     1((INDEX(J),COEN(J),SIGMCO(J),J=1,NOIN)
1315 GO TO (1316,1580),NIX
1316 GO TO NUMBER, (1320,1580)
1320 ELEVEL=VMIN*DEER/VECTOR(NOVAR,NOVAR)
1330 IF (EEOUT+ELEVEL) 1350,1350,1340
1340 K=NOMIN
1345 NOENT=0
     GO TO 1391
1350 DENOM=VECTOR(NOVAR,NOVAR)-VMAX
     IF (DENOM) 1351,1351,1352
1351 NIX=2
     GO TO 1370
1352 ELEVEL=VMAX*DEER/DENOM
1360 IF (EEIN-ELEVEL) 1370,1361,1380
1361 IF (EEIN) 1380,1380,1370
1370 K=NOMAX
1390 NOENT=K
1391 IF (K) 1392,1392,1400
1392 WRITE (6,1395) NOSTEP
1394 GO TO 910
1400 DO 1410 I=1,NOVAR
1420 IF (I-K) 1430,1410,1430
1430 DO 1440 J=1,NOVAR
1450 IF (J-K) 1460,1440,1460
1460 VECTOR(I,J)=VECTOR(I,J)-(VECTOR(I,K)*VECTOR(K,J)/VECTOR(K,K))
1440 CONTINUE
1410 CONTINUE
1470 DO 1480 I=1,NOVAR
1490 IF (I-K) 1500,1480,1500
1500 VECTOR(I,K)=-VECTOR(I,K)/VECTOR(K,K)
1480 CONTINUE
1510 DO 1520 J=1,NOVAR
1530 IF (J-K) 1540,1520,1540
1540 VECTOR(K,J)=VECTOR(K,J)/VECTOR(K,K)
1520 CONTINUE
1550 VECTOR(K,K)=1.0/VECTOR(K,K)
1560 GO TO (1000,1561),NIX
1561 WRITE(6,1004) NOSTEP
     R=1.00
     SIGY=0.0
     IESTEP=0
     GO TO 1015
1380 WRITE(6,75) NOSTEP
1381 IF (IESTEP) 900,1582,1570
1570 ASSIGN 1580 TO NUMBER
1571 GO TO 1310
1580 CONTINUE
     WRITE (6,1586) (L,VECTOR(L,L),L=1,NOVMI)
1581 IF (IERRED) 900,1582,910
1582 CONTINUE
1583 WRITE (6,83)
1586 FORMAT (24H0     DIAGONAL  ELEMENTS //20H  VAR.NO.       VALUE//
     1(1H  I 7,E16.6))
```

```
 1590 DO 1660 N=1,NODATA
 1610 YPRED=CNST
 1620 DO 1630  I=1,NOIN
 1640 K=INDEX(I)
 1630 YPRED=YPRED+COEN(I)*DATAS(N,K)
      Y(N)=YPRED
      X(N)=DATAS(N,NOVAR)
 1650 DEV=DATAS(N,NOVAR)-YPRED
      PCTDEV=DEV*100./DATAS(N,NOVAR)
      S1=S1+ABS(DATAS(N,NOVAR))
      S2=S2+ABS(YPRED)
      S3=S3+ABS(DEV)
      S4=S4+ABS(PCTDEV)
 1660 WRITE(6,80) DATAS(N,NOVAR),YPRED,DEV,PCTDEV
      S1=S1/RNODATA
      S2=S2/RNODATA
      S3=S3/RNODATA
      S4=S4/RNODATA
      WRITE(6,81) S1,S2,S3,S4
      IF(IFPLOT) 900,1635,910
 1635 ENCODE(10,1636,IN(2)) DIV,PROB,NOPROB
 1636 FORMAT (A3,A4,I3)
      ENCODE(6,1637,YAXIS) YAX
      ENCODE (6,1637,XAXIS) XAX
 1637 FORMAT (A6)
      CALL DDIPLT (1,IN,NODATA,X,Y,0,0,0,0,1,XAXIS,1,YAXIS,1,ITAPE)
  910 CONTINUE
  121 GO TO 100
 1800 WRITE (6,93) INVAR
 1801 WRITE (6,94) NOVAR
      GO TO 910
    5 FORMAT (3E10.5,3I5,1H 12I2)
    9 FORMAT (33X16HTOTAL INPUT DATA  //)
C....FORMAT 10 FOR READING INPUT DATA
   10 FORMAT (6E12.5)
   11 FORMAT (1H0/)
C....FORMAT 12 FOR WRITING INPUT DATA
   12 FORMAT (6E12.5)
   15 FORMAT (1H 49H                                          SUM  OF  VARIABLES//)
   20 FORMAT (1H 11H      SUM X( I2,3H) = E12.4,8H  SUM X( I2,3H) =E12.4,
     18H  SUM X( I2,3H) =E12.4,8H  SUM X(I2,3H) =E12.4 )
   25 FORMAT (17H       SUM    Y    =E12.4)
   30 FORMAT(1H0 70H                                  RAW  SUM  OF  SQUARES  A
     1ND  CROSS PRODUCTS// )
   35 FORMAT (1H 7H      X(I2,7H) VS X(I2,3H) = E15.6,
     1          6H     X(I2,7H) VS X(I2,3H) = E15.6,
     2          6H     X(I2,7H) VS X(I2,3H) = E15.6  )
   40 FORMAT (1H 7H      X(I2,12H) VS    Y    =E15.6,
     1          6H     X(I2,12H) VS    Y    =E15.6,
     2          6H     X(I2,12H) VS    Y    =E15.6  )
   45 FORMAT (1H 21H      Y      VS    Y    =E15.6)
   50 FORMAT (1H063H                                        AVERAGE  VALUE  OF
     1  VARIABLES// )
   55 FORMAT(1H077H                                  RESIDUAL  SUMS  OF  SQUA
     1RES  AND  CROSS PRODUCTS//)
   60 FORMAT(1H069H                                       SIMPLE  CORRELATI
     1ON  COEFFICIENTS//)
   65 FORMAT (25H0  STANDARD ERROR OF Y = E12.6 )
```

```
   70 FORMAT (11H    F LEVEL    F12.4 /25H    STANDARD ERROR OF Y     F12.4/
     135H  MULTIPLE CORRELATION COEFFICIENT     F12.5/                  12H
     2   CONSTANT F13.5/56H                VARIABLE   COEFFICIENT   STD  ERR
     3OR OF COEF     //  (16H                  X-I3,F15.5, F15.5 ))
   75 FORMAT (10H COMPLETED I5,20H STEPS OF REGRESSION)
   80 FORMAT (14X,2H  F12.5,3H    F12.5,2H  F12.5,3H  F12.5)
   81 FORMAT (1H0,1X12H     AVERAGES,2H  F12.5,3H    F12.5,2H  F12.5,2H
     1F12.5)
   85 FORMAT (1H043H                    PREDICTED VS ACTUAL RESULTS  /73H
     1                    ACTUAL         PREDICTED      DEVIATION      PCT. DE
     2V.  //)
   90 FORMAT (22H1STEPWISE  REGRESSION //12H PROBLEM NO I10 //13H NO OF
     1DATA = I5 //18H NO OF VARIABLES = I10 //30H WEIGHTED DEGREES OF FR
     2EEDOM = F12.2 //28H F LEVEL TO ENTER VARIABLE = F10.3 //29H F LEVE
     3L TO REMOVE VARIABLE = F9.3  /// )
   91 FORMAT (9H0STEP NO.I5 /19H    VARIABLE REMOVED I8)
   92 FORMAT (9H0STEP NO.I5 /20H    VARIABLE ENTERING I8)
   93 FORMAT (45H1INVAR SHOULD NOT BE GREATER THAN  50.  IT IS I5)
   94 FORMAT (45H1NOVAR SHOULD NOT BE GREATER THAN  50.  IT IS I5)
  654 FORMAT (31H  ZERO NUMBER OF DATA. SO LONG.)
  905 FORMAT (42H ERROR IN CONTROL CARD, PROBLEM TERMINATED)
  906 FORMAT (25H ERROR, VMIN PLUS. SOLONG)
  907 FORMAT (26H  ERROR,NOIN MINUS, SOLONG )
 1004 FORMAT (1H037HY SQUARE NON-POSITIVE,TERMINATE STEP  I 5)
 1019 FORMAT (1H029H NO MORE DEGREES FREEDOM STEP I 5 )
 1044 FORMAT (1H010H SQUARE X-I5,17H NEGATIVE. SOLONG I5,6H STEPS)
 1395 FORMAT (12H  K=0. STEP I6, 7H SOLONG)
      END
```

REFERENCES

1. Maahs, Howard G.; and Schryer, David R.: Chemical Impurity Data on Selected Artificial Graphites With Comments on the Catalytic Effect of Impurities on Oxidation Rate. NASA TN D-4212, 1967.

2. Maahs, Howard G.: Effects of Natural Chemical Impurities and Crystallite Orientation on the Erosion Behavior of Artificial Graphite. NASA TN D-6023, 1970.

3. Maahs, Howard G.: Crystallographic Data on Selected Artificial Graphites With Comments on the Role of the Degree of Crystal Development in Oxidation. NASA TN D-4888, 1968.

4. Nightingale, R. E.; Yoshikawa, H. H.; and Losty, H. H. W.: Physical Properties. Nuclear Graphite, R. E. Nightingale, ed., Academic Press, Inc., 1962, pp. 117-194.

5. Rappeneau, J.; Bocquet, M.; Fillatre, A.; and Trutt, J. C.: Permeabilite aux Gaz des Graphites Nucleaires—Etude de la Structure Poreuse par Porosimetrie au Mercure. Proceedings of the Fifth Conference on Carbon, Vol. 1, Pergamon Press, Inc., 1962, pp. 335-353.

6. Barrett, Elliott P.; Joyner, Leslie G.; and Halenda, Paul P.: The Determination of Pore Volume and Area Distributions in Porous Substances. I. Computations From Nitrogen Isotherms. J. Amer. Chem. Soc., vol. 73, Jan. 1951, pp. 373-380.

7. Moore, Walter J.: Physical Chemistry. Third ed., Prentice-Hall, Inc., 1962.

8. Shull, C. G.: The Determination of Pore Size Distribution From Gas Adsorption Data. J. Amer. Chem. Soc., vol. 70, Apr. 1948, pp. 1405-1410.

9. Anon.: The Industrial Graphite Engineering Handbook. Union Carbide Corp., c.1960, pp. 5B.01.01-5B.01.06.

10. Mayo, Robert F.; Wells, William L.; and Wallio, Milton A.: A Magnetically Rotated Electric Arc Air Heater Employing a Strong Magnetic Field and Copper Electrodes. NASA TN D-2032, 1963.

11. Fay, J. A.; and Riddell, F. R.: Theory of Stagnation Point Heat Transfer in Dissociated Air. J. Aeronaut. Sci., vol. 25, no. 2, Feb. 1958, pp. 73-85, 121.

12. Exton, Reginald J.: Theory and Operation of a Variable Exposure Photographic Pyrometer Over the Temperature Range 1800° to 3600° F (1255° to 2255° K). NASA TN D-2660, 1965.

13. Wilson, R. Gale; and Spitzer, Cary R.: Visible and Near-Infrared Emittance of Ablation Chars and Carbon. AIAA J., vol. 6, no. 4, Apr. 1968, pp. 665-671.

14. Null, M. R.; and Lozier, W. W.: Research and Development on Advanced Graphite Materials – Vol. XXI. Carbon Arc Image Furnace Studies of Graphite. WADD-TR-61-72, Vol. XXI, U.S. Air Force, Nov. 1963. (Available from DDC as AD No. 426 665.)

15. Box, George E. P.; Cousins, Wilfred R.; Davies, Owen L.; Himsworth, Francis R.; Kenney, Harold; Milbourn, Maurice; Spendley, William; and Stevens, Wilfred L.: Statistical Methods in Research and Production With Special Reference to the Chemical Industry. Owen L. Davies, ed., Hafner Pub. Co., 1961.

16. Efroymson, M. A.: Step-Wise Multiple Regression. SHARE Program Catalog SDA No. 3143, June 10, 1964.

17. Maahs, Howard G.; and Schryer, David R.: Particle Removal in the Ablation of Artificial Graphite. AIAA J., vol. 7, no. 11, Nov. 1969, pp. 2178-2179.

18. Slosarik, S. E.; and Swope, L. M.: Relationship of Graphite Properties to Rocket Nozzle Erosion. Paper presented at the Sixth Biennial Conference on Carbon (Pittsburgh, Pa.), June 1963.

19. Chase, M. J.: Erosion Resistant Graphites for Solid Propellant Rocket Motors. Paper presented at the Eighth Biennial Conference on Carbon (Buffalo, N.Y.), June 1967.

20. McVey, D. F.; Auerbach, I.; and McBride, D. D.: Some Observations on the Influence of Graphite Microstructure on Ablation Performance. AIAA Paper No. 70-155, Jan. 1970.

21. Yahr, G. T.; and Witt, F. J.: A Test for Determining the Thermal Shock Resistance of Graphites. Paper presented at the Eighth Biennial Conference on Carbon (Buffalo, N.Y.), June 1967.

TABLE I.- MATERIAL-PROPERTY AND ABLATION-PERFORMANCE DATA

Graphite	Bulk density, ρ_p, g/cm^3	Air displacement density, ρ_{air}, g/cm^3	Theoretical density, ρ_T, g/cm^3	Total pore, volume, V_p, cm^3/g	Most probable pore radius, R_p, μm	Maximum grain size, G_m, mm	Pore volume, v_p, cm^3/g	Pore area, A_p, m^2/g	Surface area, S, m^2/g	Average pore radius, r_a, Å	Most probable micropore radius, r_p, Å	Mean pore radius, r_m, Å
AHDG	1.877	2.041	2.257	0.066	[a] 1.77	0.84	0.0033	1.2	1.4	100	15	49.4
ME 11	1.627	2.114	2.255	.157	2.36	.076	.0025	1.0	1.2	108	15	43.6
ME 14	1.735	2.067	2.256	.091	1.74	.076	.0027	.9	1.0	120	14	53.7
ME 15	1.739	2.077	2.245	.091	2.01	.18	.0029	1.2	1.3	100	15	45.7
ME 18	1.592	2.153	2.255	.149	2.42	.076	.0026	.9	1.1	109	15	49.2
H-205	1.783	2.095	2.251	.088	6.55	.41	.0021	.8	.8	120	14	52.3
H-205-85	1.835	2.053	2.248	.069	4.74	.15	.0023	.8	.8	124	15	56.0
MHLM	1.777	2.089	2.259	.095	15.2	.84	.0021	.7	.8	127	15	53.0
MHLM-85	1.857	2.043	2.259	.082	[a] 2.13	.84	.0025	.9	1.0	111	15	50.1
2BE	1.514	2.159	2.257	.205	2.13	.15	.0029	1.1	1.2	112	15	50.6
2D8D	1.480	2.074	2.230	.196	1.77	.18	.0042	1.7	1.8	102	15	47.6
2D9B	1.689	1.974	2.252	.097	2.13	.18	.0032	1.3	1.4	101	15	46.6
W119	1.739	2.078	2.257	.095	1.16	.25	.0054	1.9	2.1	118	15	54.0
L-56	1.607	2.070	2.232	.142	3.55	.15	.0024	1.0	1.1	119	9	50.3
L-56-GP	1.603	2.075	2.234	.144	3.22	.15	.0024	.9	1.0	125	12	51.5
P-3W	1.661	2.071	2.257	.137	1.84	.15	.0049	1.5	1.7	138	15	60.5
P-3W-GP	1.640	2.058	2.258	.136	1.87	.15	.0043	1.3	1.5	134	14	61.7
E-24	1.566	2.100	2.232	.157	3.88	.13	.0027	1.1	1.3	76	16	42.5
3499	1.680	2.110	2.259	.135	3.22	.076	.0040	1.4	1.6	109	17	52.9
3499-S	1.590	2.183	2.258	.177	4.09	.076	.0056	1.7	2.0	133	15	58.6
39-RL	1.631	2.189	2.258	.159	2.84	.076	.0051	1.8	2.0	115	15	53.2
4007	1.661	2.158	2.259	.150	5.35	.20	.0063	1.9	2.1	139	15	60.7
8827	1.764	2.120	2.259	.107	2.53	.076	.0038	1.1	1.2	143	15	63.7
9-RL	1.667	2.212	2.259	.142	3.81	.076	.0062	1.9	2.1	134	15	60.9
9050	1.777	2.090	2.258	.097	3.44	.076	.0024	.9	1.0	104	17	51.3
L1	1.539	2.105	2.255	.192	2.73	.15	.0031	1.2	1.3	114	16	52.4
L31	1.606	2.075	2.231	.136	4.63	.15	.0016	1.1	1.0	94	8	41.9
331	1.705	2.084	2.257	.106	1.19	.076	.0035	1.0	1.2	134	15	57.7
AGSX	1.645	2.173	2.259	.152	1.69	.41	.0033	1.2	1.4	113	15	50.6
ATJ	1.717	2.062	2.257	.112	3.55	.15	.0020	.7	.6	91	13	43.8
ATJ-GP	1.709	2.070	2.258	.100	2.96	.15	.0030	.9	1.1	118	14	52.3
ATJS	1.837	2.052	2.257	.076	[a] 1.06	.15	.0022	1.0	1.0	101	15	44.9
ATJS-GP	1.825	2.026	2.257	.077	[a] 1.11	.15	.0035	1.1	1.3	123	15	57.8
ATL	1.791	2.077	2.258	.089	[a] 1.06	.76	.0023	1.0	1.0	98	15	46.3
ATL-GP	1.776	2.073	2.258	.091	[a] 1.63	.76	.0028	1.0	1.1	124	13	54.0
CDA	1.654	2.195	2.257	.150	4.34	.15	.0024	.9	1.0	121	15	52.3
CDG	1.503	2.151	2.255	.214	6.45	.41	.0029	.9	1.0	124	15	56.3
CDG-GP	1.491	2.284	2.257	.239	5.35	.41	.0061	1.4	1.6	156	18	76.7
CMB	1.810	1.978	2.257	.044	.43	.076	.0026	1.1	1.2	107	12	47.0
PGR	1.688	2.096	2.259	.122	[a] 1.33	.76	.0030	.9	1.0	143	14	58.5
AGOT	1.736	2.182	----	.115	2.13	.76	-----	---	---	---	---	---
AXF-5Q	1.803	2.208	----	.095	.44	.025	-----	---	---	---	---	---
Graph-i-tite "A"	1.897	2.165	----	.050	[a] .54	.84	-----	---	---	---	---	---
Graph-i-tite "G" (0.840)	1.908	2.050	----	.060	[a] .54	.84	-----	---	---	---	---	---
Graph-i-tite "G" (0.203)	1.873	2.015	----	----	----	.203	-----	---	---	---	---	---

[a] Best estimate. No definite most probable size.

[b] None detected.

[c] Specimen lost during run. Length estimated from film record.

TABLE I.- MATERIAL-PROPERTY AND ABLATION-PERFORMANCE DATA – Concluded

Graphite	Total void porosity, ϵ, %	Air-open void porosity, θ_{air}, %	Mercury-open void porosity, θ_{Hg}, %	Ash content, $\overline{A}$, ppm	Interlayer spacing, d_c, Å	Thermal conductivity, k, W/cm-K	Specimen length change, $\Delta\ell$, cm	Surface temperature, T, K	Recession rate, $\dot{s}$, cm/sec	Surface texture, τ	Degree of deformation, Γ
AHDG	16.8	8.0	12.4	1132	3.361	1.444	0.3686	2178	0.01432	2	2
ME 11	27.9	23.0	25.5	417	3.364	.641	.5072	2189	.01726	1	1
ME 14	23.1	16.1	15.8	254	3.363	.694	.4298	2161	.01586	1	1
ME 15	22.6	16.3	15.8	123	3.379	.465	.4486	2161	.01715	1	1
ME 18	29.4	26.1	23.7	362	3.364	.523	.5222	2183	.01802	1	1
H-205	20.8	14.9	15.7	1519	3.370	1.226	.4356	2206	.01763	1	2
H-205-85	18.4	10.6	12.7	4150	3.375	1.119	.3881	2178	.01707	1	2
MHLM	21.4	14.9	16.9	742	3.358	1.454	.6495	2233	.02576	3	2
MHLM-85	17.8	9.1	15.2	692	3.359	1.573	.5197	2239	.02310	3	2
2BE	32.9	29.9	31.0	1119	3.361	.683	.5626	2228	.02001	1	2
2D8D	33.6	28.6	29.0	2491	3.403	.184	.7866	2283	.02003	1	2
2D9B	25.0	14.4	16.4	3197	3.369	.423	.5596	2261	.01782	1	1
W119	23.0	16.3	16.5	4226	3.361	.479	.5057	2233	.01873	1	1
L-56	28.0	22.4	22.8	(b)	3.399	.446	.4572	2100	.01793	1	1
L-56-GP	28.2	22.8	23.1	(b)	3.396	.460	.4790	2144	.01726	1	1
P-3W	26.4	19.8	22.8	(b)	3.361	.832	.4295	2061	.01734	1	1
P-3W-GP	27.4	20.3	22.3	3	3.360	.836	.4285	2044	.01648	1	1
E-24	29.8	25.4	24.6	932	3.399	.400	.6172	2222	.02227	1	3
3499	25.6	20.4	22.7	466	3.359	1.237	.4943	2183	.01970	1	1
3499-S	29.6	27.2	28.1	460	3.360	1.076	.4948	2122	.01642	1	1
39-RL	27.8	25.5	25.9	(b)	3.360	1.162	.4816	2128	.01840	1	1
4007	26.5	23.0	24.9	380	3.359	.942	.4829	2172	.01955	2	3
8827	21.9	16.8	18.9	419	3.358	1.191	.4097	2094	.01733	1	1
9-RL	26.2	24.6	23.7	(b)	3.359	1.191	.4001	2083	.01795	1	1
9050	21.3	15.0	17.2	391	3.360	1.240	.3947	2061	.01454	1	1
L1	31.8	26.9	29.5	709	3.364	.673	.5278	2111	.01912	1	1
L31	28.0	22.6	21.8	377	3.400	.460	.5415	2150	.01767	1	2
331	24.4	18.2	18.1	1476	3.362	.537	.4917	2167	.01836	1	1
AGSX	27.2	24.3	25.0	580	3.359	1.313	.6284	2183	.02668	3	3
ATJ	23.9	16.7	19.2	1209	3.361	.970	.4559	2200	.01718	1	1
ATJ-GP	24.3	17.4	17.1	25	3.360	.908	.3835	2139	.01582	1	1
ATJS	18.6	10.5	14.0	1625	3.361	1.153	.3985	2161	.01533	1	1
ATJS-GP	19.2	9.9	14.1	(b)	3.361	1.175	.3668	2061	.01447	1	1
ATL	20.7	13.8	15.9	5810	3.360	1.037	.6606	2300	.02092	3	3
ATL-GP	21.3	14.3	16.2	17	3.360	1.034	.7142	2256	.03072	3	3
CDA	26.7	24.7	24.8	709	3.361	.812	.4882	2189	.01888	1	1
CDG	33.4	30.1	32.2	531	3.364	.801	.9385	2211	.02826	2	3
CDG-GP	33.9	34.7	35.6	(b)	3.362	.819	.7435	2178	.02235	2	3
CMB	19.8	8.5	8.0	64	3.362	.380	.4178	2139	.01554	1	1
PGR	25.3	19.5	20.6	688	3.358	.781	[c] 1,0460	2244	.04287	3	3
AGOT	---	20.4	20.0	[d] 740	----	[d] 1.450	.5319	2200	.02252	3	2
AXF-5Q	---	18.4	17.1	[d] 150	----	[d] <.796	.4567	2156	.02162	1	1
Graph-i-tite "A"	---	12.4	9.5	[d] <600	----	[d] .949	.3719	2206	.01468	2	3
Graph-i-tite "G" (0.840)	---	6.9	11.4	[d] <600	----	[d] 1.068	[e] .3297	[e] 2200	[e] .01259	[e] 2	[e] 2
Graph-i-tite "G" (0.203)	---	7.1	---	370	----	[d] 1.126	(f)	(f)	(f)	[e] 1	[e] 1

[d] Obtained from manufacturer's literature.

[e] Also see additional ablation data in table II.

[f] See table II for ablation data.

TABLE II.- COMPARISON OF Graph-i-tite "G" ABLATION PERFORMANCE FOR DIFFERENT GRAIN SIZES

[Nominal heating rate = 562 W/cm^2]

Material	Total recession in 30 seconds, Δl, cm	Recession rate, $\dot{s}$, cm/sec	Surface temperature, T, K
Graph-i-tite "G" (G_m = 0.840 mm)	0.3289	0.01461	2050
	.3147	.01327	2010
Graph-i-tite "G" (G_m = 0.203 mm)	0.3358	0.01458	1980
	.3366	.01423	1970
	.3457	.01341	1950
ATJ	0.4224	0.01757	2120

TABLE III.- CRITERIA FOR ELIMINATING GRAPHITES FROM CONSIDERATION BASED ON $\Gamma \leq 1.5$

Maximum grain size, G_m, mm	Calculated density below which if the actual bulk density of a graphite falls, it is to be eliminated, g/cm^3
0.84	2.20
.76	2.13
.41	1.84
.25	1.72
.203	1.68
.20	1.68
.18	1.66
.15	1.64
.13	1.62
.076	1.58
.025	1.54

TABLE IV.- ABLATION PERFORMANCE PREDICTIONS AT 1-PERCENT SIGNIFICANCE LEVEL

Graphite	Δl, cm		T, K		$\dot{s}$, cm/sec		τ		Γ	
	Predicted	Measured	Predicted	Measured	Predicted	Measured	Predicted	Measured	Predicted	Measured
Equations (16) to (20)										
AGOT	0.6952	0.5319	2207	2200	0.02645	0.02252	2.8	3	2.7	2
AXF-5Q	.3080	.4567	>2123	2156	.01328	.02162	.8	1	.7	1
Graph-i-tite "A"	.5715	.3719	<2251	2206	.02428	.01468	3.0	2	2.4	3
Graph-i-tite "G" (0.840 mm)	.5607	.3297	<2243	2200	.02404	.01259	3.0	2	2.4	2
Equations (21) to (23)										
[a] AXF-5Q	(b)	0.4567	(b)	2156	0.01604	0.02162	(c)	1	(c)	1

[a] From correlations for graphites with the requirements that $\tau \leqq 1.3$ ($G_m \leqq 0.22$ mm) and $\Gamma \leqq 1.5$ (criteria in table III) at the 2.5-percent significance level.

[b] No prediction possible because r_m not available.

[c] Not applicable.

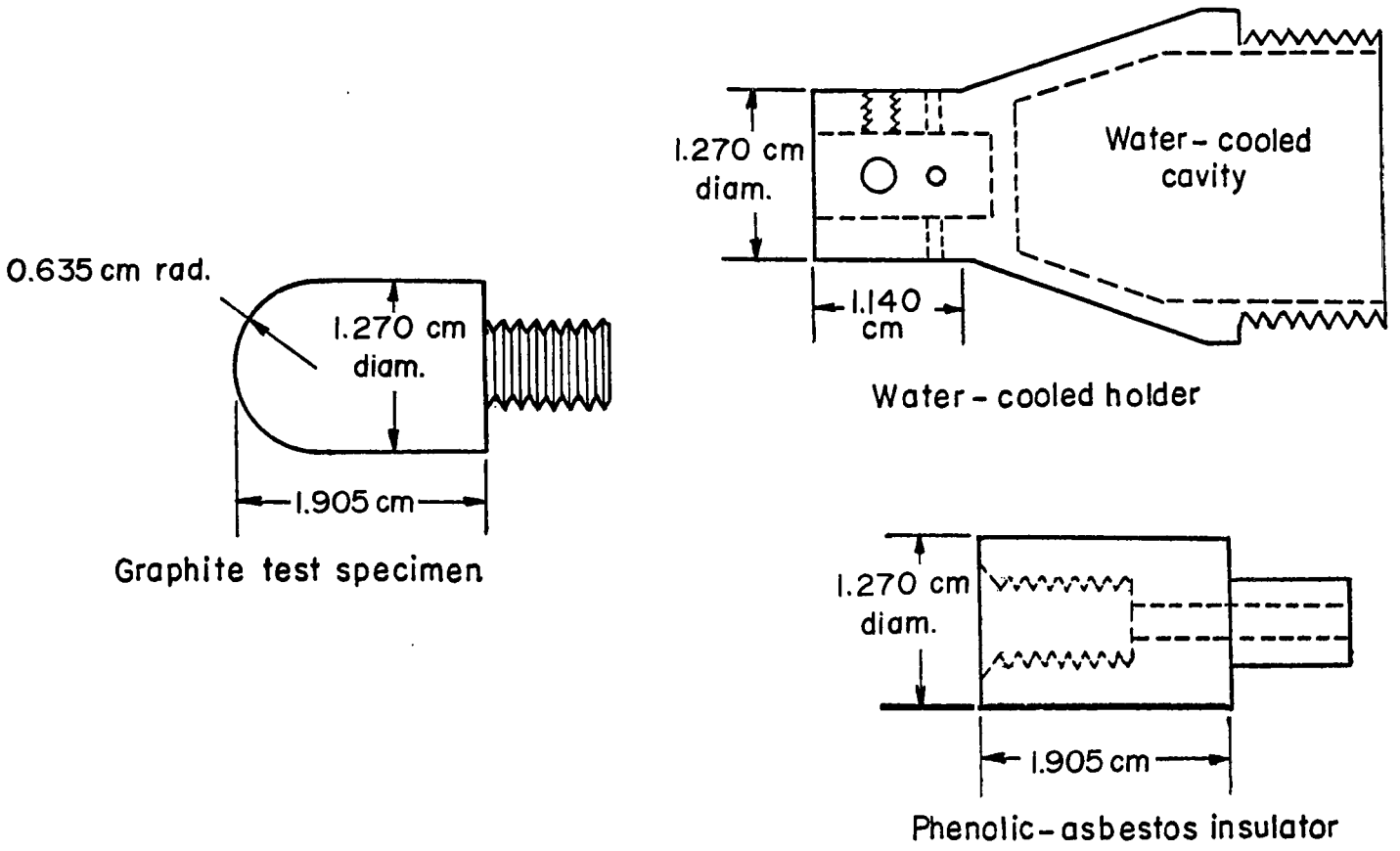

Figure 1.- Schematic drawing showing graphite test specimen, water-cooled holder, and insulator.

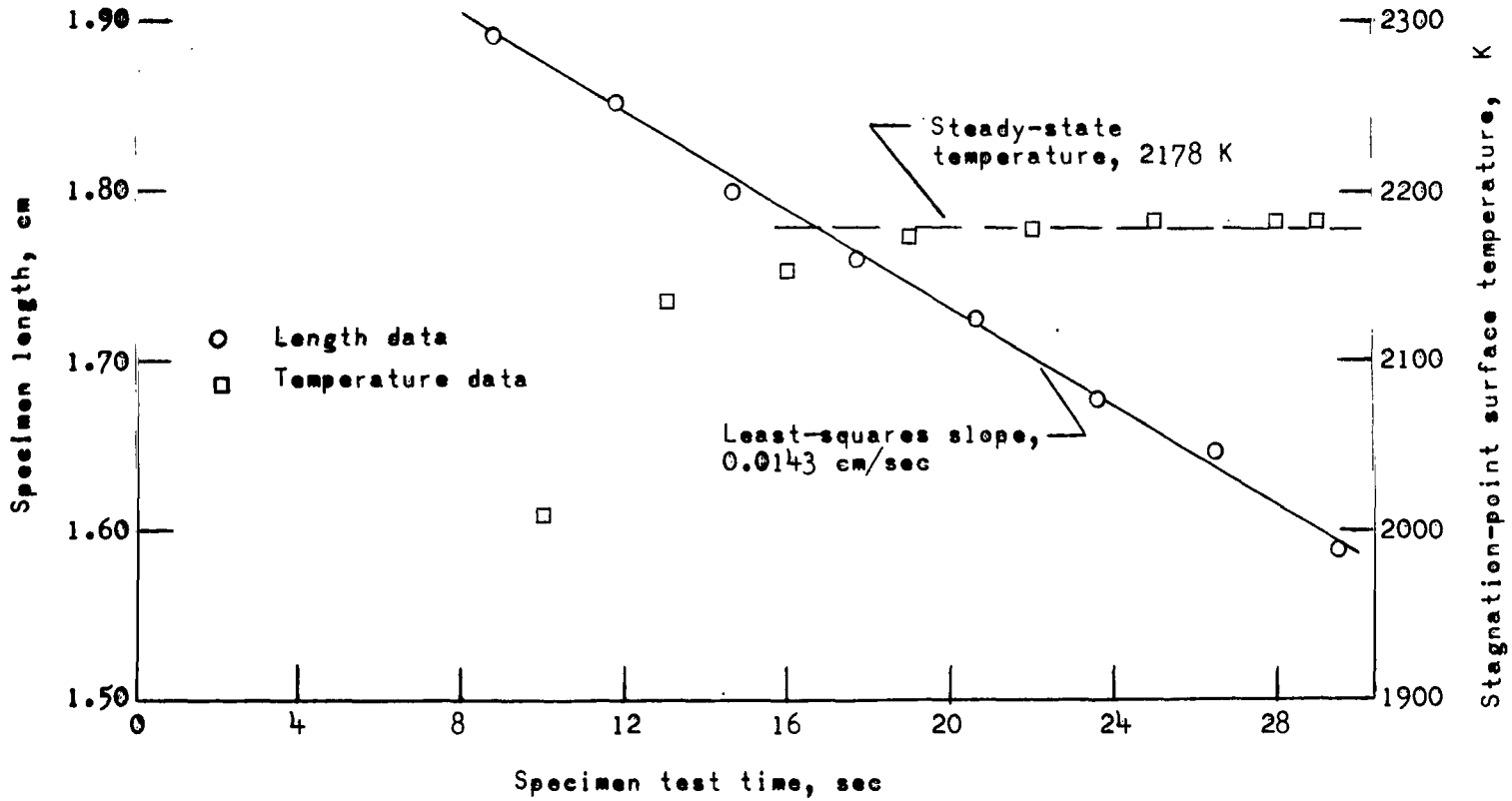

Figure 2.- Sample plot of specimen length and surface temperature as a function of time (AHDG graphite).

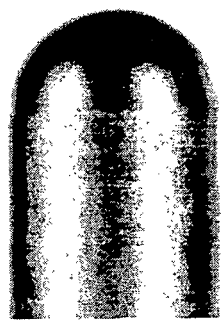

Untested

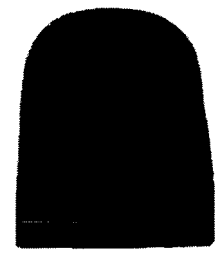

τ = 1 (smooth)

Γ = 1 (no gouging)

τ = 2 (slightly rough)

Γ = 3 (severe gouging)

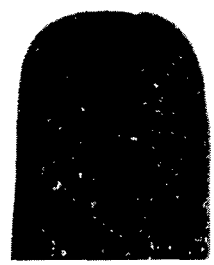

τ = 2 (slightly rough)

Γ = 2 (slight gouging)

τ = 3 (rough)

Γ = 2 (slight gouging)

L-72-116

Figure 3.- Photograph of representative after-test specimens indicating the quantitative assignation of surface texture τ and degree of gouging Γ.

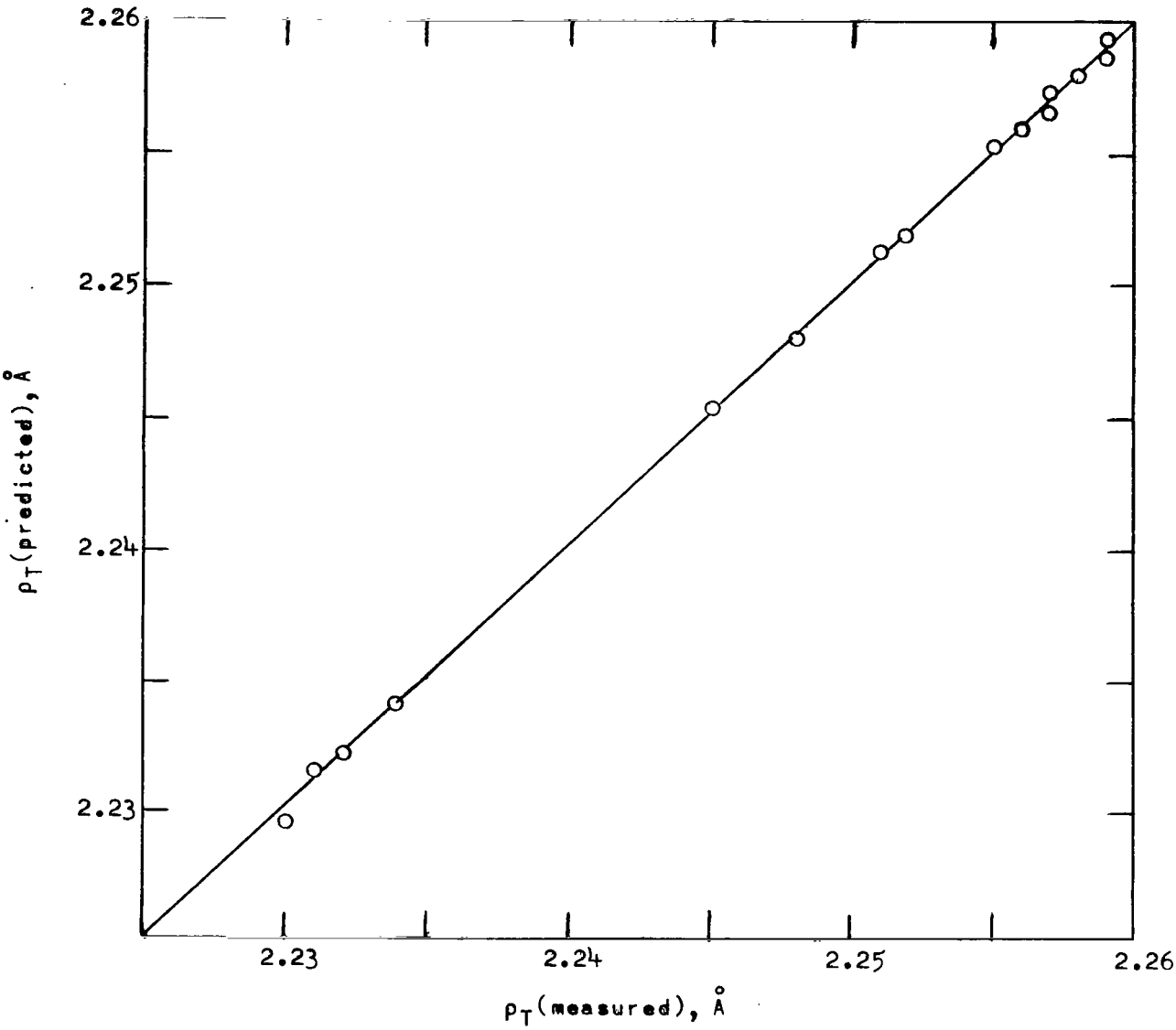

(a) Theoretical density, equation (1).

Figure 4.- Comparison of measured values of material properties with values predicted by correlations.

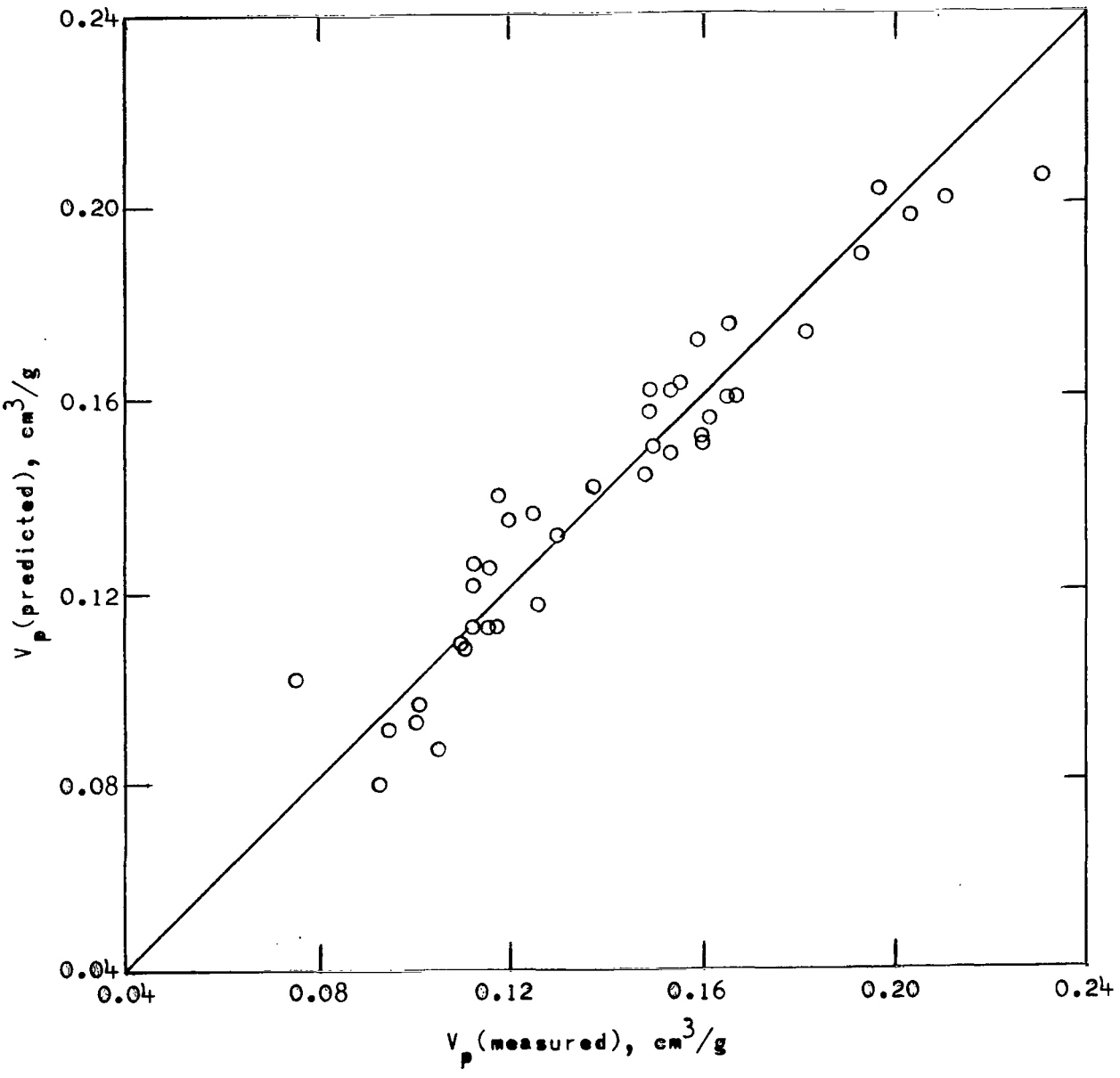

(b) Total pore volume, equation (2).

Figure 4.- Continued.

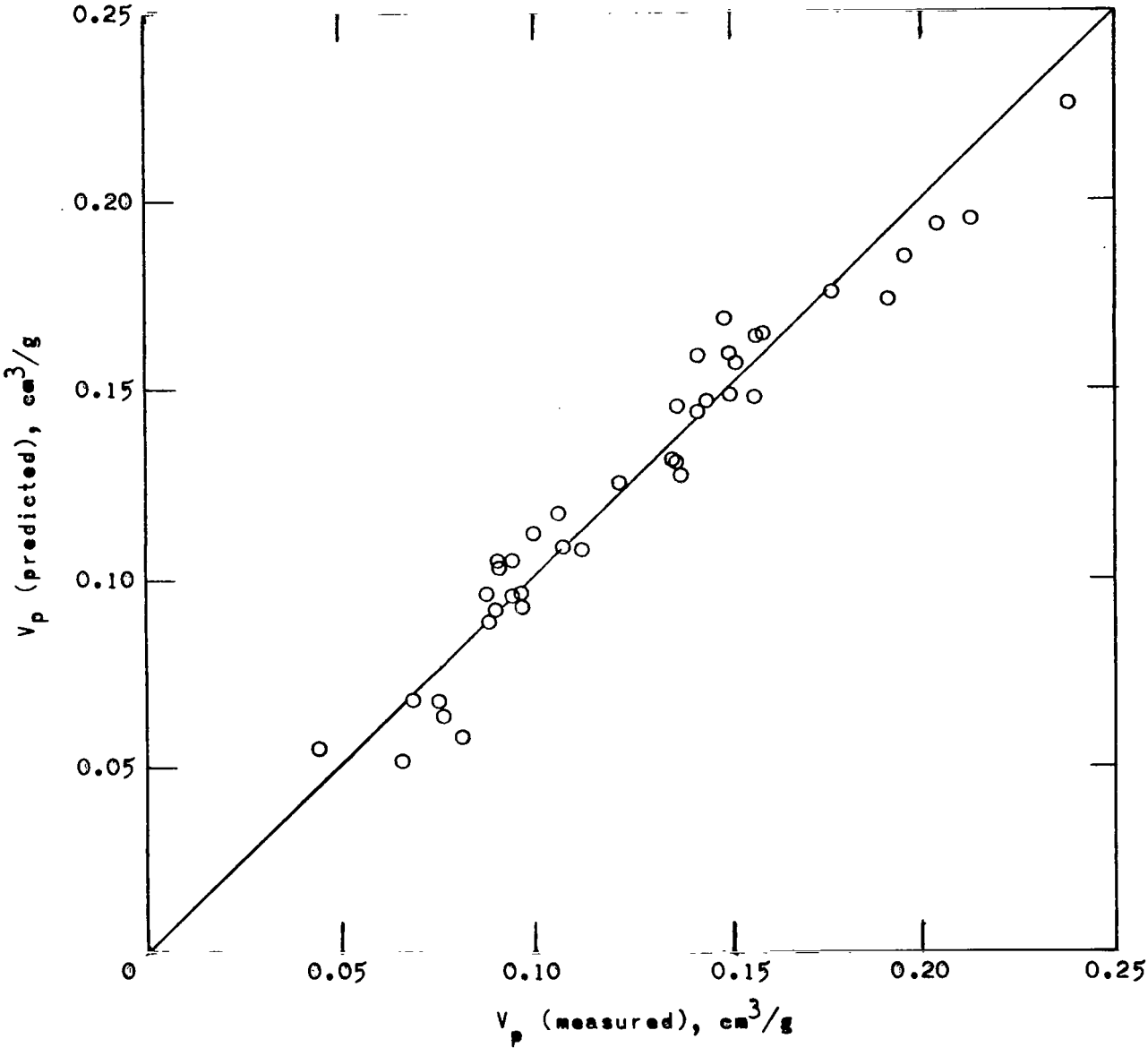

(c) Total pore volume, equation (3).

Figure 4.- Continued.

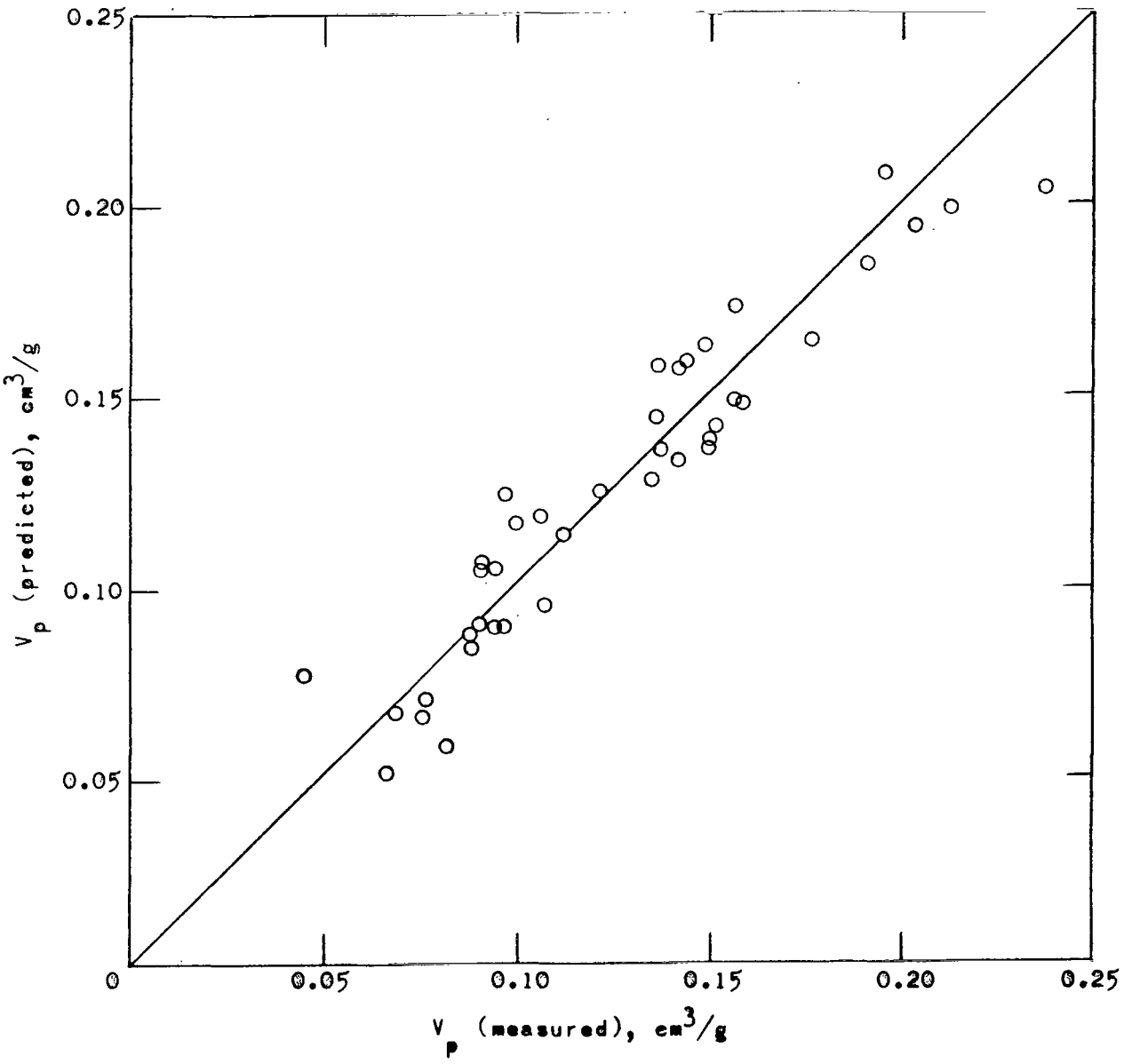

(d) Total pore volume, equation (4).

Figure 4.- Continued.

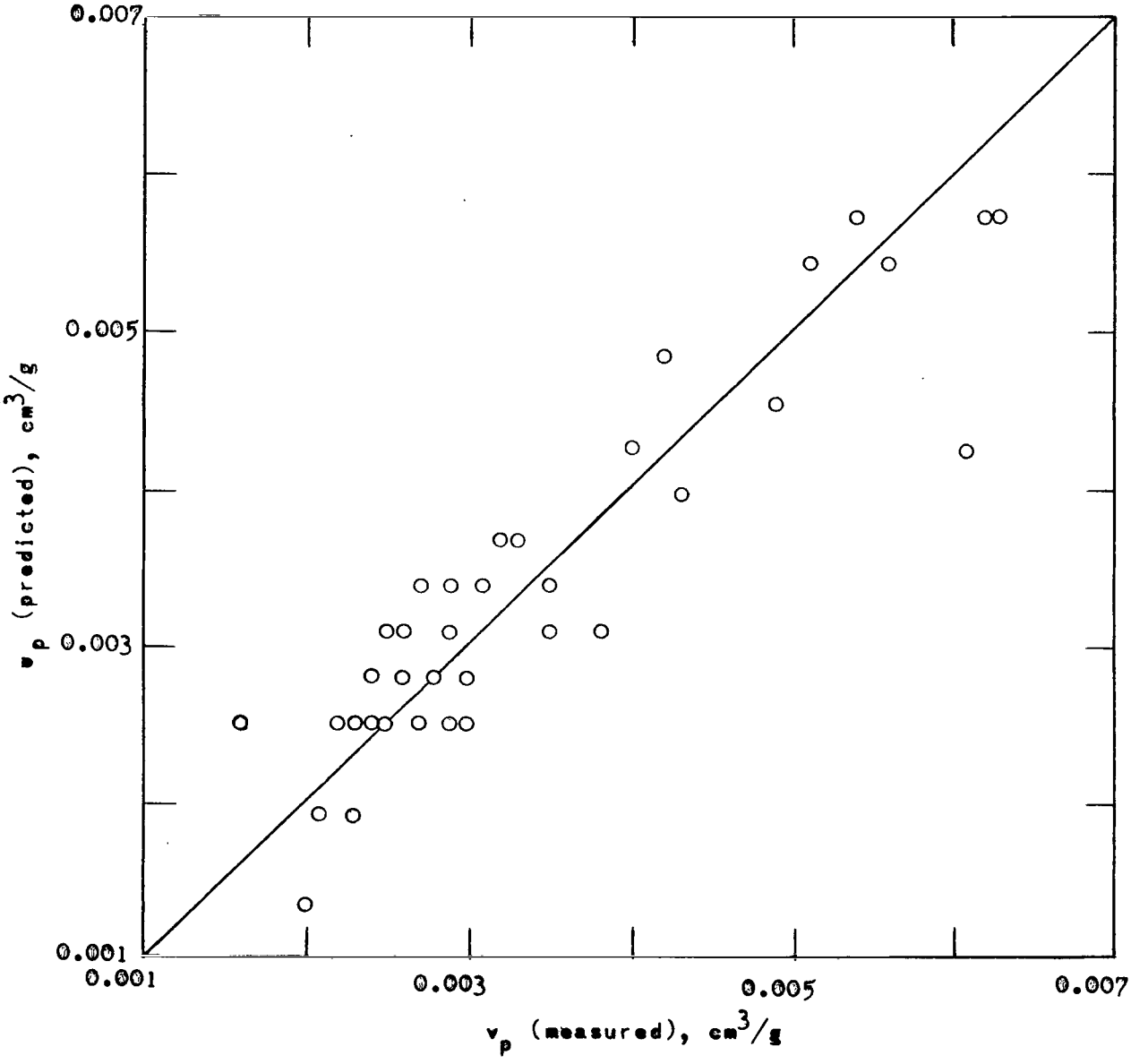

(e) Pore volume, equation (5).

Figure 4.- Continued.

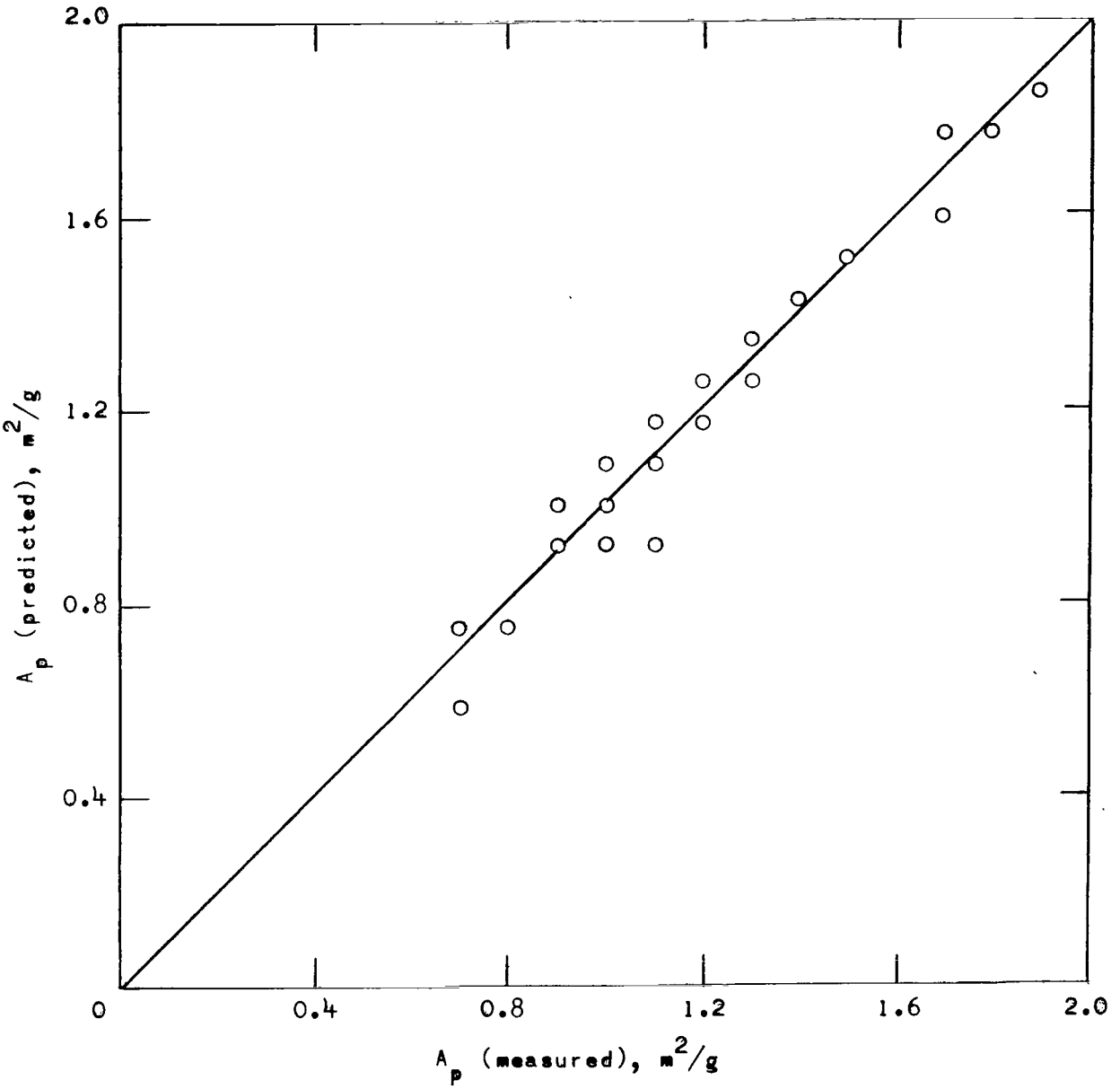

(f) Pore area, equation (6).

Figure 4.- Continued.

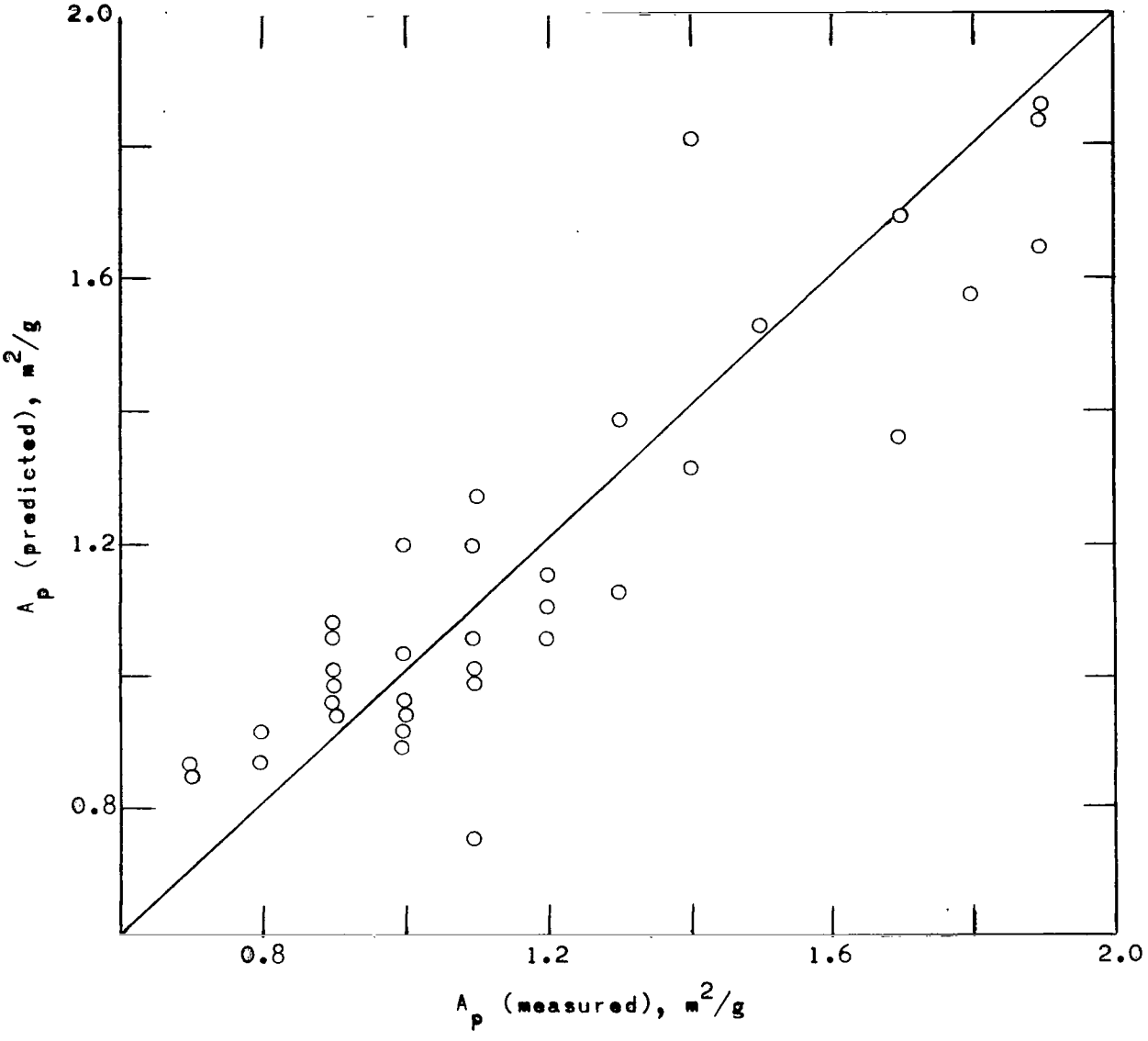

(g) Pore area, equation (7).

Figure 4.- Continued.

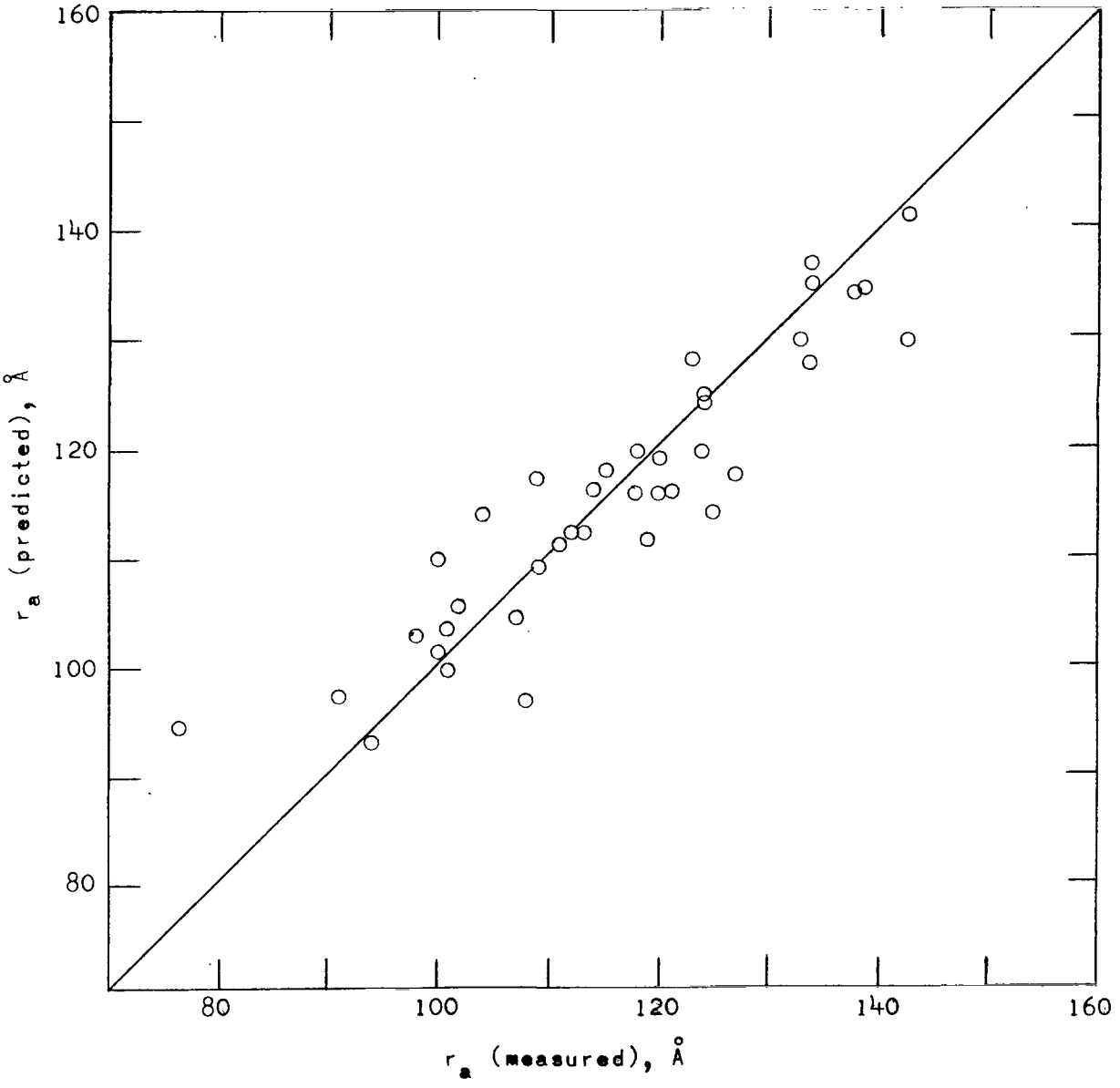

(h) Average pore radius, equation (8).

Figure 4.- Continued.

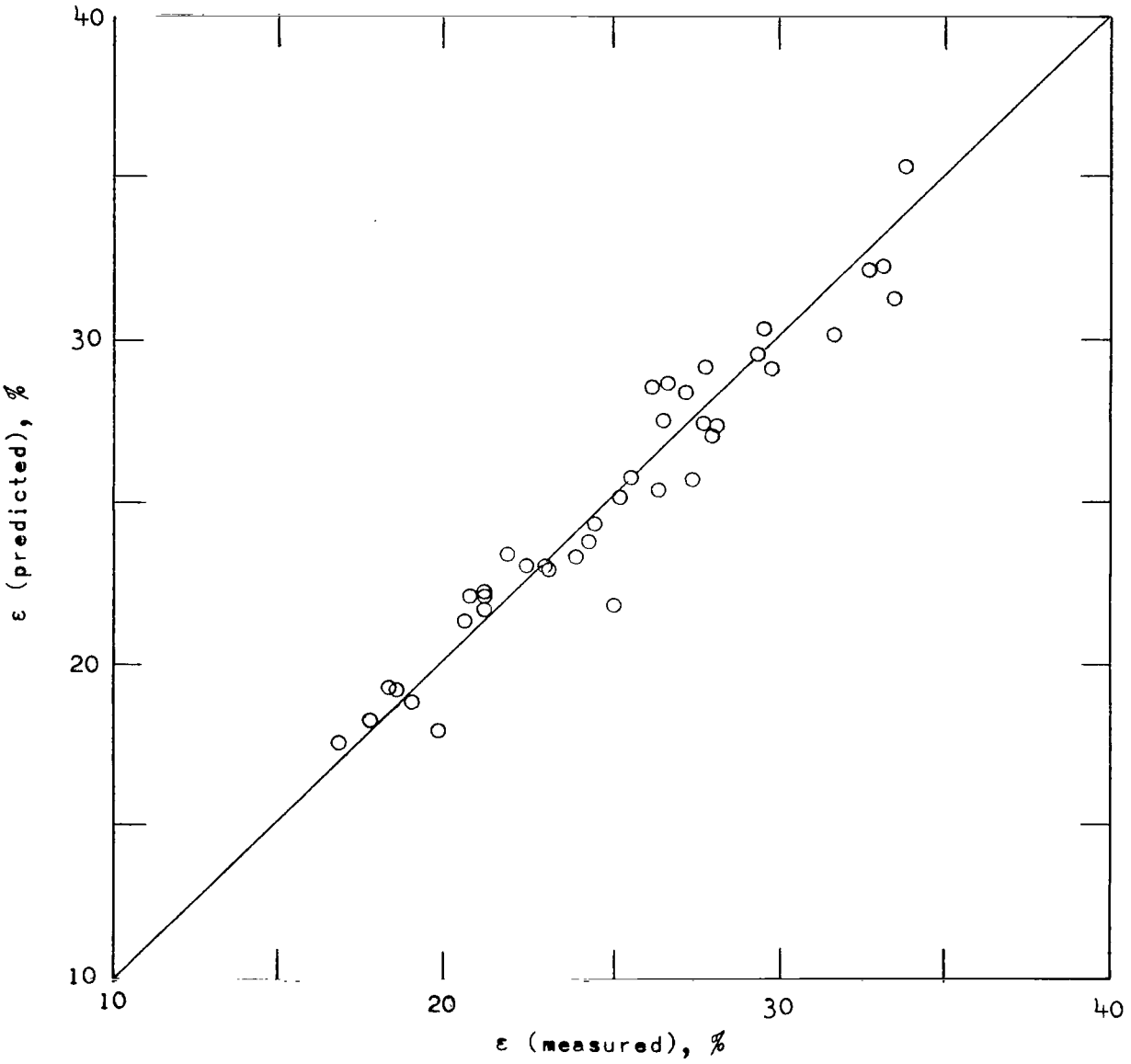

(i) Total void porosity, equation (9).

Figure 4.- Continued.

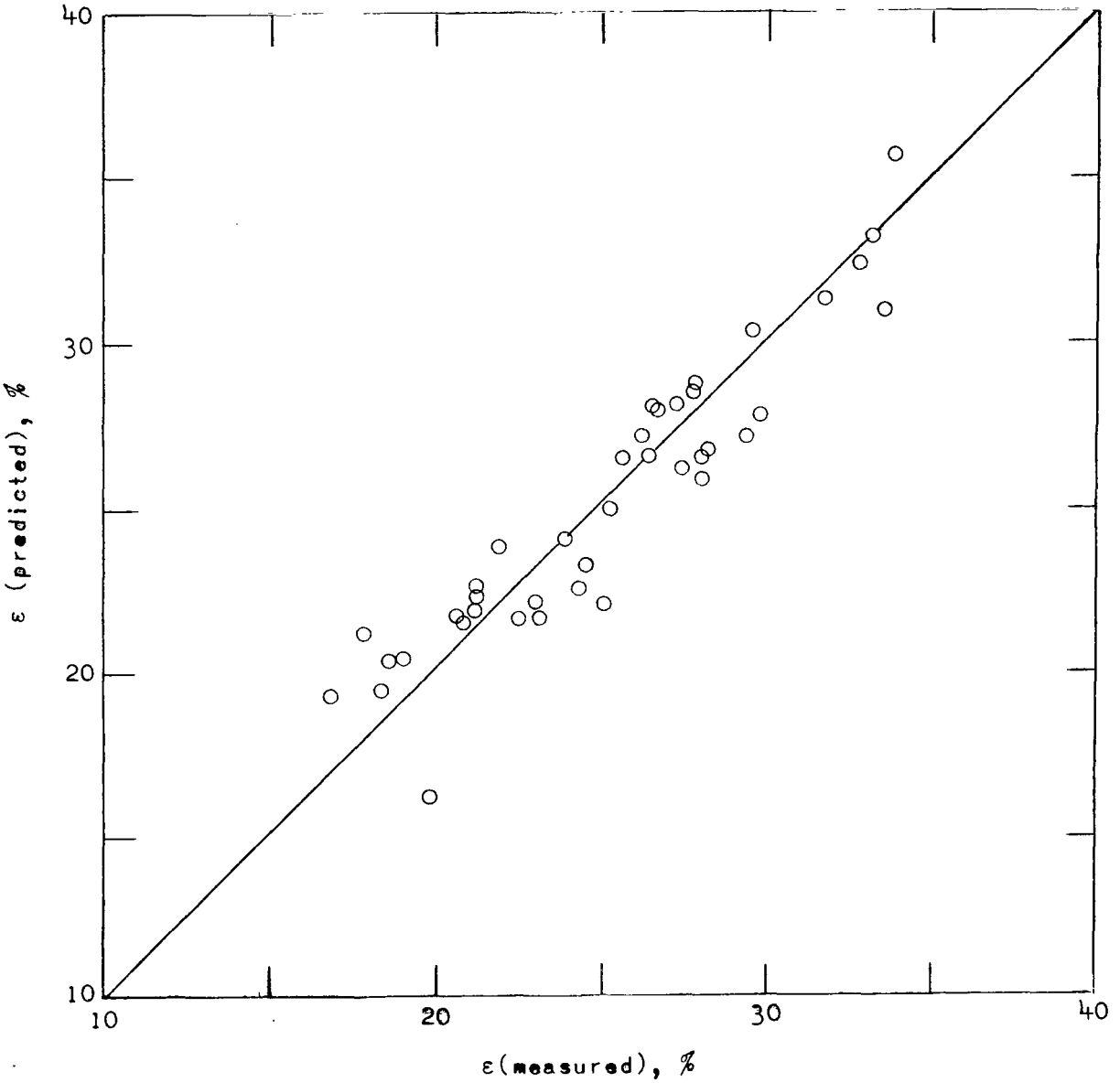

(j) Total void porosity, equation (10).

Figure 4.- Continued.

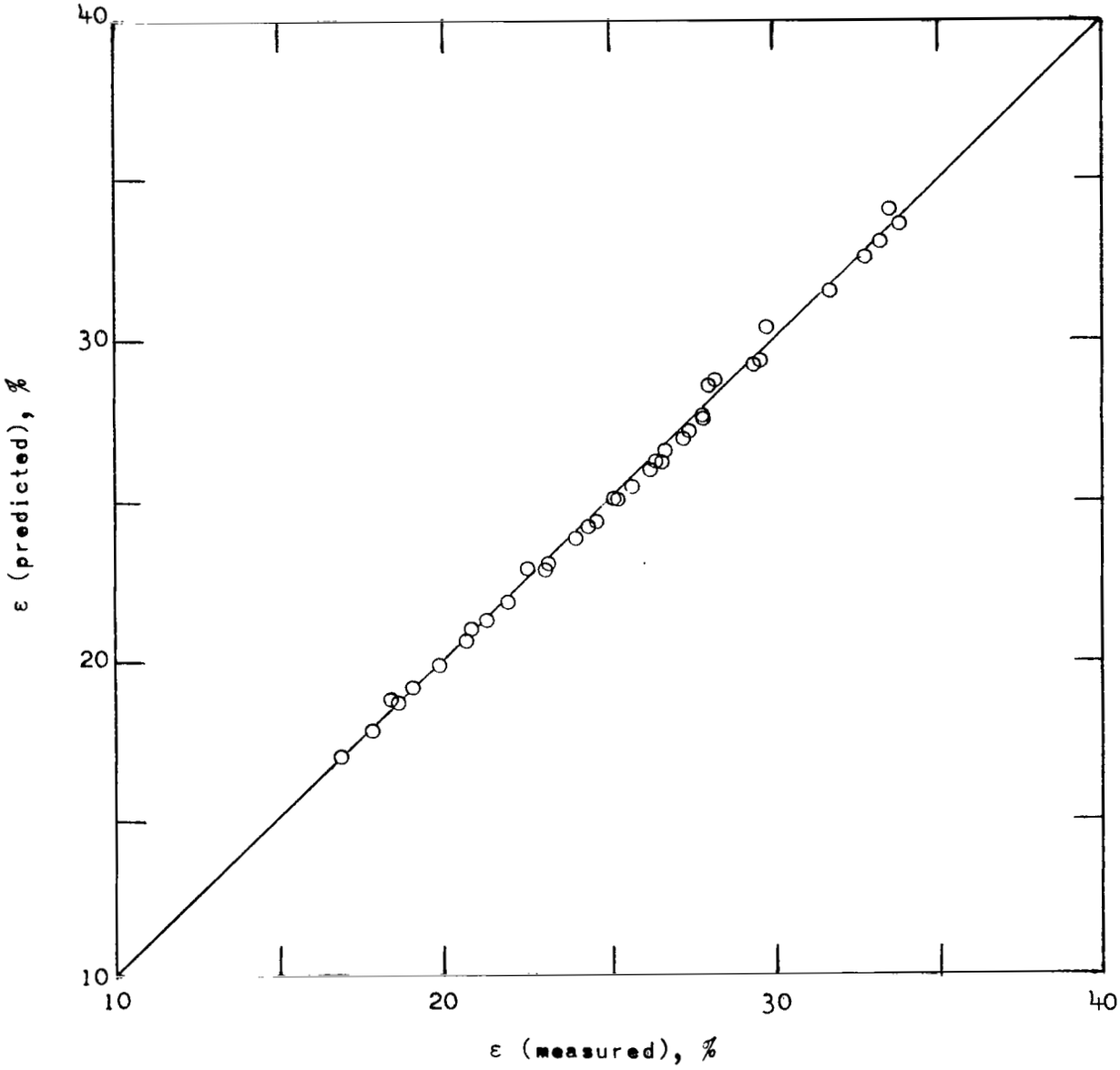

(k) Total void porosity, equation (11).

Figure 4.- Continued.

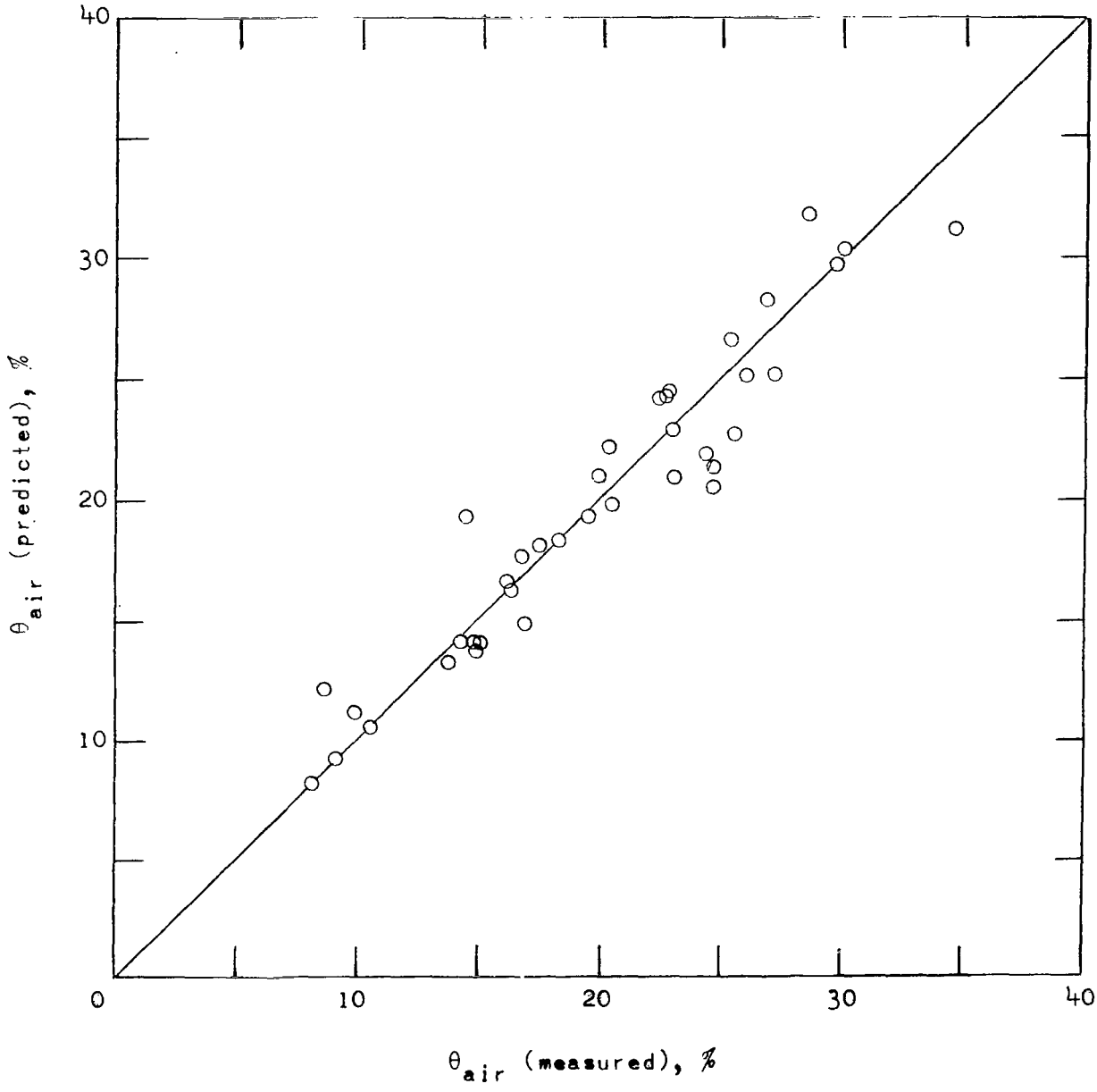

(l) Air-open void porosity, equation (12).

Figure 4.- Continued.

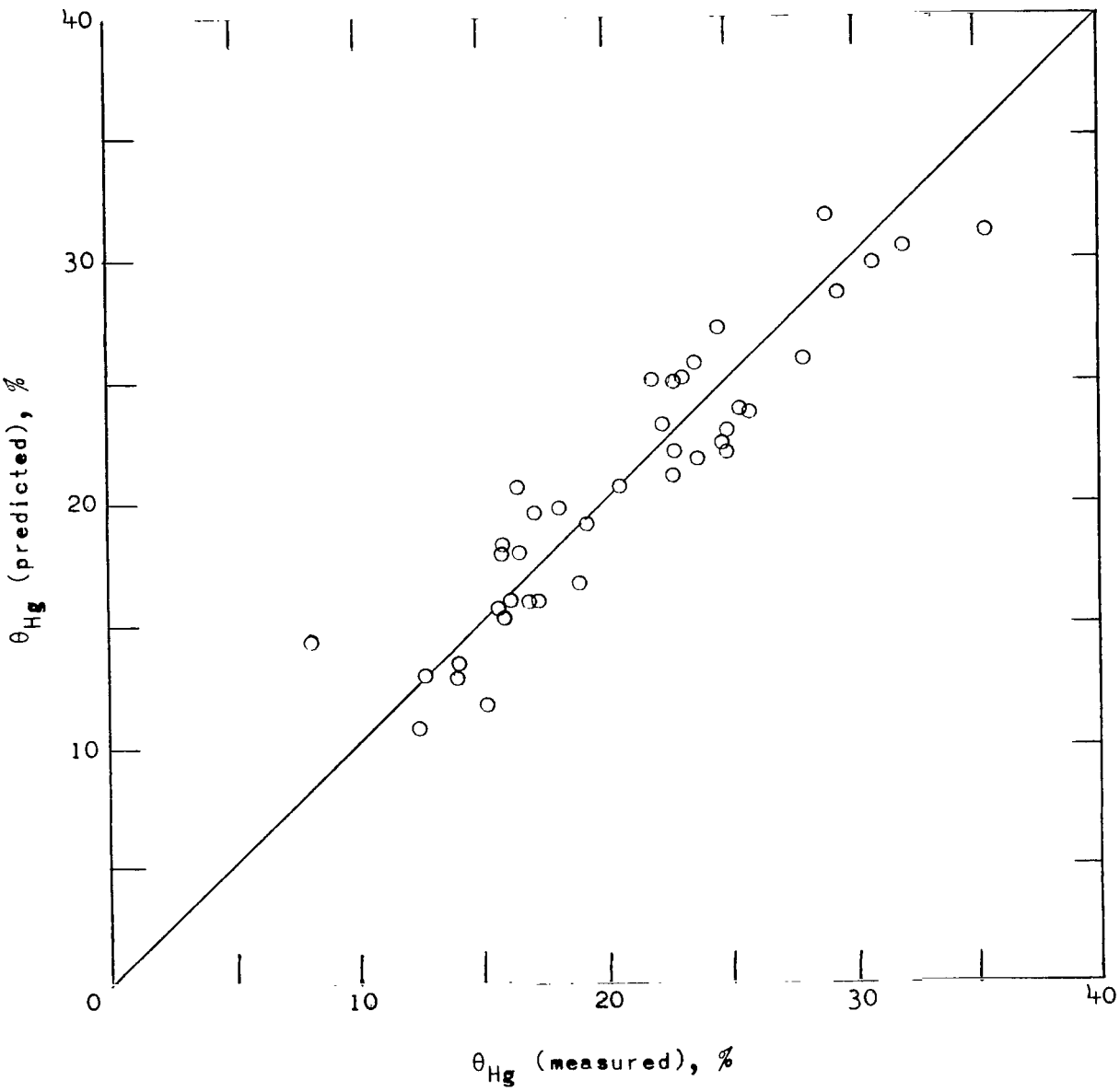

(m) Mercury-open void porosity, equation (13).

Figure 4.- Continued.

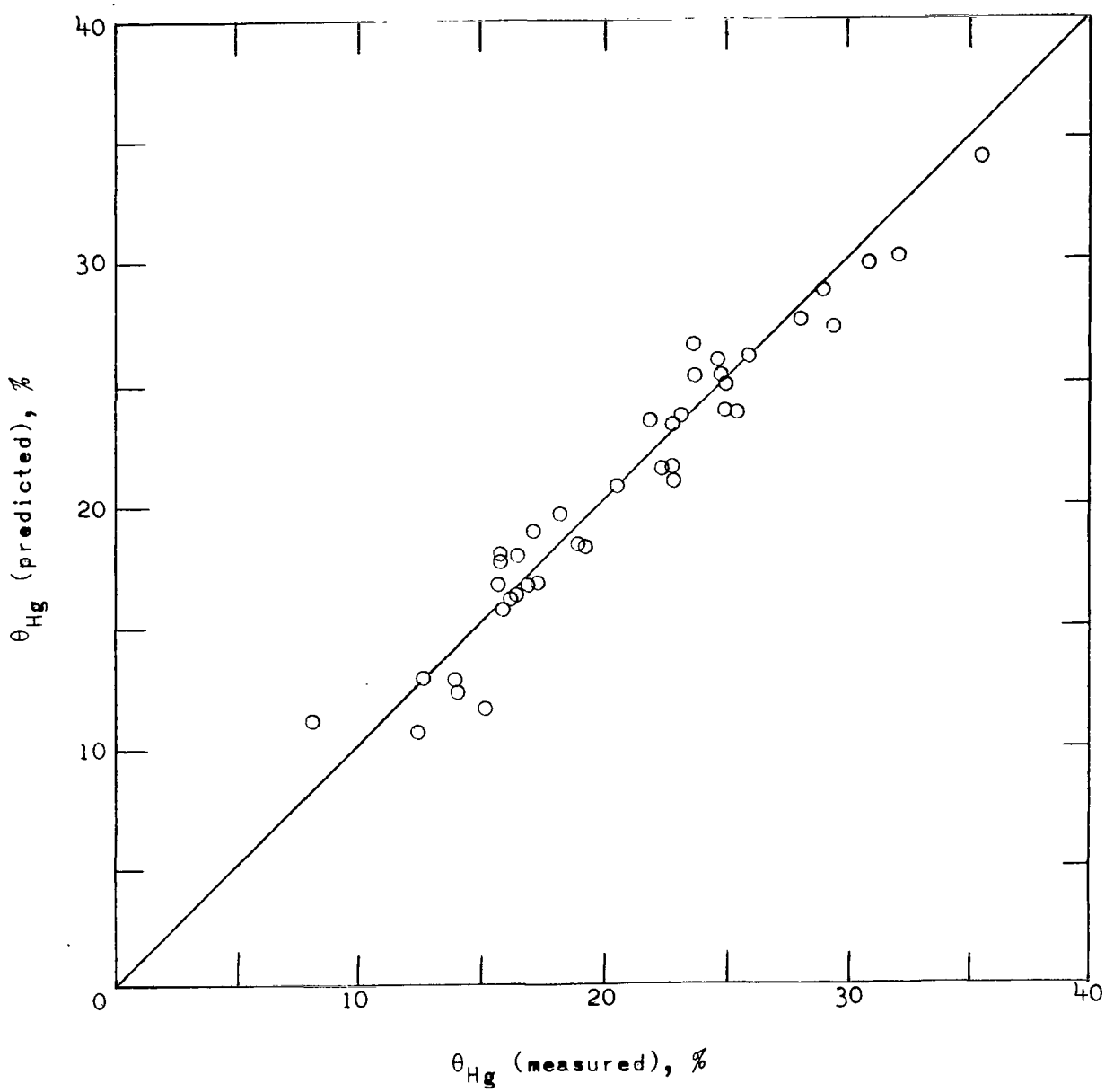

(n) Mercury-open void porosity, equation (14).

Figure 4.- Continued.

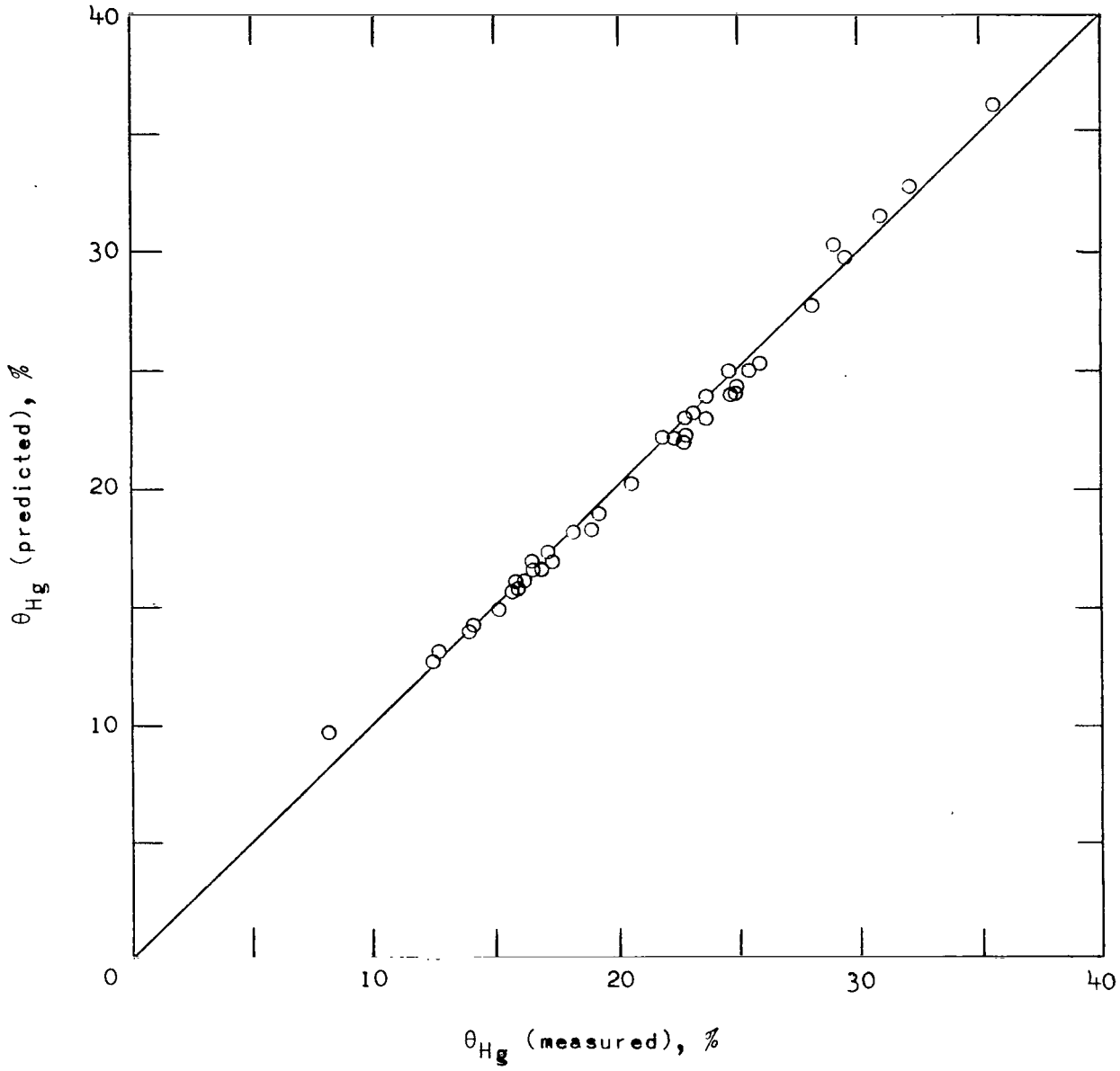

(o) Mercury-open void porosity, equation (15).

Figure 4.- Concluded.

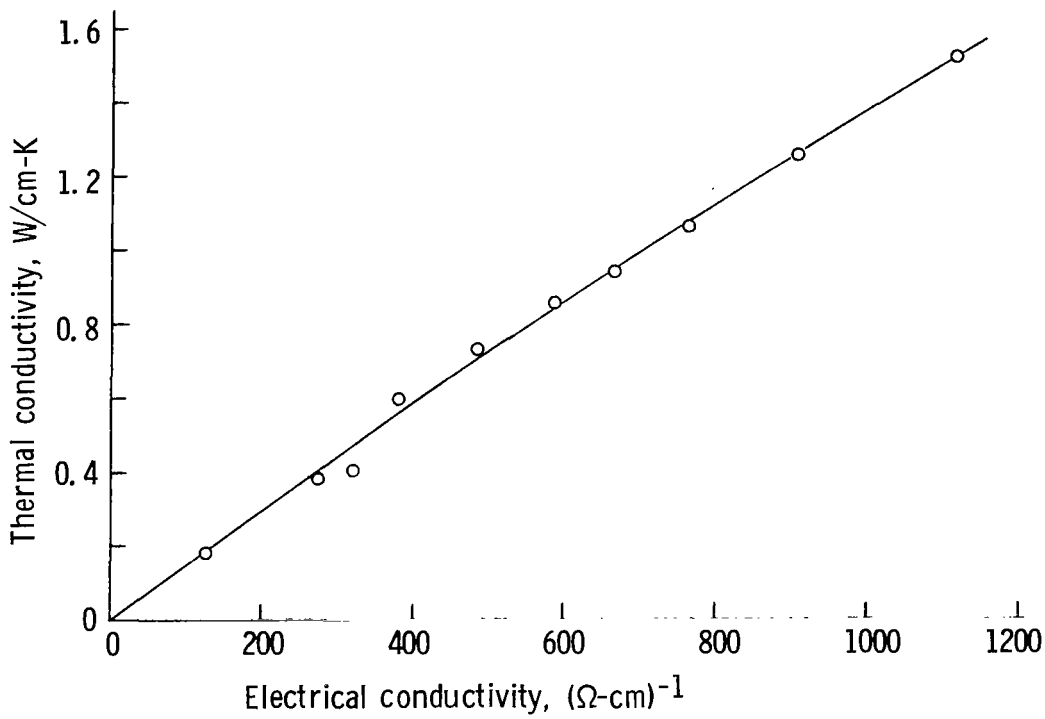

Figure 5.- Thermal conductivity as a function of electrical conductivity.

NASA-Langley, 1972 —— 33 L-8085

"The aeronautical and space activities of the United States shall be conducted so as to contribute . . . to the expansion of human knowledge of phenomena in the atmosphere and space. The Administration shall provide for the widest practicable and appropriate dissemination of information concerning its activities and the results thereof."

—NATIONAL AERONAUTICS AND SPACE ACT OF 1958

NASA SCIENTIFIC AND TECHNICAL PUBLICATIONS

TECHNICAL REPORTS: Scientific and technical information considered important, complete, and a lasting contribution to existing knowledge.

TECHNICAL NOTES: Information less broad in scope but nevertheless of importance as a contribution to existing knowledge.

TECHNICAL MEMORANDUMS: Information receiving limited distribution because of preliminary data, security classification, or other reasons.

CONTRACTOR REPORTS: Scientific and technical information generated under a NASA contract or grant and considered an important contribution to existing knowledge.

TECHNICAL TRANSLATIONS: Information published in a foreign language considered to merit NASA distribution in English.

SPECIAL PUBLICATIONS: Information derived from or of value to NASA activities. Publications include conference proceedings, monographs, data compilations, handbooks, sourcebooks, and special bibliographies.

TECHNOLOGY UTILIZATION PUBLICATIONS: Information on technology used by NASA that may be of particular interest in commercial and other non-aerospace applications. Publications include Tech Briefs, Technology Utilization Reports and Technology Surveys.

Details on the availability of these publications may be obtained from:

SCIENTIFIC AND TECHNICAL INFORMATION OFFICE

NATIONAL AERONAUTICS AND SPACE ADMINISTRATION

Washington, D.C. 20546